Multichannel parametrization of πN scattering amplitudes and extraction of resonance parameters

M. Shrestha and D. M. Manley
Department of Physics, Kent State University, Kent, Ohio 44242-0001, USA
(Received 17 August 2012; published 29 November 2012)

We present results of a new multichannel partial-wave analysis for πN scattering in the c.m. energy range 1080 to 2100 MeV. This work explicitly includes ηN and $K\Lambda$ channels and the single pion photoproduction channel. Resonance parameters were extracted by fitting partial-wave amplitudes from all considered channels using a multichannel parametrization that is consistent with S-matrix unitarity. The resonance parameters so obtained are compared to predictions of quark models.

DOI: 10.1103/PhysRevC.86.055203 PACS number(s): 13.75.Gx, 14.20.Gk, 13.30.Eg, 11.80.Et

I. INTRODUCTION

According to quark models, nucleons (baryons) are bound states of three constituent quarks. The excited states of these quarks give rise to the baryon resonance spectrum. There are many models [1–5] that describe the interactions between the quarks in baryons. In spite of all these different approaches, they pose the same common scenario: a greater number of predicted states as compared to the experimentally verified states. As an example, only nine N^* resonances have been confirmed by experimental analyses (as listed by the Particle Data Group (PDG) [6]) whereas at least 21 states are predicted in the same energy range [5]. The possible reason for the discrepancy is either the models are based on wrong assumptions or the analyses for the extraction of resonance information are incomplete. In this work we focus on the second possibility.

Almost all analyses [7,8] use the study of πN elastic scattering as the main source for the extraction of N^* resonance parameters. Information on the coupling of resonances to other channels has come mainly from analyses of πN inelastic scattering. This might be the reason for the missing states as the πN channel is predicted to decouple from many resonances with masses above 1.7 GeV [9]. It is thus logical to look for resonances in other inelastic channels including photoproduction channels at the higher energies. An analysis that incorporates all possible channels simultaneously is highly desirable.

Currently, other groups working on analyses of πN scattering are the EBAC group [10], the Bonn-Gatchina Group [11], and the GWU/SAID [12] group. The EBAC group uses a dynamical coupled-channels approach. The channels included are πN, $\pi\pi N$, ηN, $K\Lambda$, and γN. The group of Huang *et al.* [13] has also used a dynamical coupled-channels model to investigate pion photoproduction. The Bonn-Gatchina Group uses a multichannel Breit-Wigner and K-matrix approach for the amplitude parametrization; channels included are πN, $\pi\pi N$, ηN, and photoproduction channels. The SAID group maintains up-to-date partial-wave analyses (PWAs) of several reactions including $\pi N \to \pi N$ and $\gamma N \to \pi N$. Currently, they have started to use a multichannel PWA giving equal importance to the inelastic channels.

Our approach is different and unique in the sense that it uses a generalized energy-dependent Breit-Wigner parametrization of amplitudes treating all the channels on an equal footing and taking full account of non resonant backgrounds. The channels included in this analysis are πN, $\pi\pi N$, ηN, $K\Lambda$, and γN. We begin with an energy-dependent model for fitting of the πN partial-wave data. Our detailed partial-wave analyses of reactions $\pi^- p \to \eta n$ and $\pi^- p \to K^0\Lambda$ are presented elsewhere [14]. The reliability of the energy-dependent amplitudes extracted from this work is tested by using the fitted amplitudes to compare with various observables [15]. Our solution is in good agreement with available data for $\pi^- p \to \eta n$ and $\pi^- p \to K^0\Lambda$.

II. THEORETICAL ASPECTS

The KSU model, developed by Manley [16], employs a unitary multichannel parametrization to extract resonance parameters. Lee has reviewed the KSU model as one of the available models for analyzing data from meson production reactions [17]. He has shown that it can be derived starting from very general coupled-channel equations. The KSU model developed as a variation of the parametrization used in the analysis by Manley and Saleski [18] for fitting $\pi N \to \pi N$ and $\pi N \to \pi\pi N$ amplitudes. The results presented in this paper supersede those of Ref. [18]. The KSU model in its present form has been used to extract N^* and Δ^* parameters from a combined fit of $\pi N \to \pi N$, $\pi N \to \pi\pi N$, and $\gamma N \to \pi N$ amplitudes [19]. It has also been successfully applied to extract Λ^* and Σ^* parameters from multichannel fits of $\bar{K}N$ scattering amplitudes [20,21].

In the KSU model, the partial-wave S matrix is defined as

$$S = B^T R B = I + 2iT, \qquad (1)$$

where T is the corresponding partial-wave T matrix. Here R is a unitary, symmetric, and generalized multichannel Breit-Wigner matrix while B and its transpose B^T are unitary matrices describing nonresonant background. The background matrix B is constructed from a product of unitary matrices: $B = B_1 B_2 \cdots B_n$, where n is a very small integer. Further details about the background parametrization can be found in Ref. [16]. The pure resonant and background matrices T_R and T_B can be constructed as

$$T_R = (R - I)/2i; \quad T_B = (B^T B - I)/2i. \qquad (2)$$

TABLE I. Resonance parameters for states with isospin $I = 1/2$. Column 1 lists the resonance name followed by its fitted mass (in MeV) and fitted total width (in MeV). Column 2 lists the decay channel (see text for explanation). Column 3 lists the partial width in MeV and column 4 lists the corresponding branching fraction. Column 5 lists the resonant amplitude (see text).

Resonance	Channel	Γ_i (MeV)	$\mathcal{B}_i$ (%)	$\sqrt{xx_i}$
$P_{11}(1440)$	πN	161(3)	64.8(9)	+0.648(9)
1412(2)	$(\pi\Delta)_P$	16(2)	6.5(8)	+0.21(1)
248(5)	$\rho_1 N$	3(1)	1.3(4)	+0.09(1)
	σN	68(4)	27(1)	+0.42(1)
$D_{13}(1520)$	πN	73(1)	62.7(5)	+0.627(5)
1512.6(5)	$(\pi\Delta)_S$	11(1)	9.3(7)	−0.24(1)
117(1)	$(\pi\Delta)_D$	7(1)	6.3(5)	−0.20(1)
	$(\rho_3 N)_S$	24(1)	20.9(7)	−0.36(1)
	σN	<1	<1	+0.04(1)
$S_{11}(1535)$	πN	52(1)	37(1)	+0.37(1)
1538(1)	ηN	58(4)	41(2)	+0.39(1)
141(4)	$(\pi\Delta)_D$	3(1)	1.8(8)	+0.08(2)
	$(\rho_3 N)_D$	12(2)	8(1)	−0.18(1)
	$\rho_1 N$	14(1)	10(1)	−0.19(1)
	σN	2(1)	1.5(5)	+0.07(1)
	πN^*	<1	<1	+0.01(2)
$S_{11}(1650)$	πN	71(3)	57(2)	+0.57(2)
1664(2)	ηN	26(3)	21(2)	−0.34(1)
126(3)	$K\Lambda$	11(1)	8(1)	−0.22(1)
	$(\pi\Delta)_D$	9(2)	7(2)	+0.20(2)
	$(\rho_3 N)_D$	<1	<1	−0.04(2)
	$\rho_1 N$	8(2)	6(1)	−0.19(2)
	σN	<1	<1	+0.04(2)
	πN^*	<1	<1	+0.02(3)
$D_{15}(1675)$	πN	56(1)	38.6(6)	+0.386(6)
1679(1)	ηN	<1	<1	+0.03(1)
145(4)	$K\Lambda$	<1	<1	−0.03(1)
	$(\pi\Delta)_D$	66(3)	46(1)	+0.42(1)
	$(\rho_3 N)_D$	<1	<1	−0.03(1)
	$\rho_1 N$	<1	<1	+0.02(1)
$F_{15}(1680)$	πN	85.6(7)	68.0(5)	+0.680(5)
1682.7(5)	ηN	1.2(4)	1.0(3)	+0.08(1)
126(1)	$K\Lambda$	<1	<1	−0.01
	$(\pi\Delta)_P$	13(1)	10.5(9)	−0.27(1)
	$(\pi\Delta)_F$	1.2(2)	1.0(1)	+0.08(1)
	$(\rho_3 N)_P$	9.3(9)	7.4(7)	−0.22(1)
	$(\rho_3 N)_F$	3.0(3)	2.4(3)	−0.13(1)
	σN	12(1)	9.4(8)	+0.25(1)
$D_{13}(1700)$	πN	1.5(3)	2.8(5)	+0.028(5)
1665(3)	$(\pi\Delta)_S$	17(6)	31(9)	−0.09(2)
56(8)	$(\pi\Delta)_D$	2(1)	3(2)	+0.03(1)
	$(\rho_3 N)_S$	21(4)	38(6)	−0.10(1)
	σN	13(4)	24(6)	+0.08(1)
$F_{17}(1990)$	πN	4(2)	2(1)	+0.02(1)
1990(45)	$K\Lambda$	1(1)	<1	−0.010(3)
203(161)				
$D_{15}(2060)$	πN	26(10)	9(2)	+0.09(2)
2116(21)	ηN	<3	<1	+0.01(2)
307(112)	$K\Lambda$	<2	<1	+0.00(3)
	$(\pi\Delta)_D$	123(39)	40(13)	+0.19(4)
	$(\rho_3 N)_D$	<25	<9	−0.06(3)
	$\rho_1 N$	63(40)	21(15)	−0.13(5)

Resonance	Channel	Γ_i (MeV)	$\mathcal{B}_i$ (%)	$\sqrt{xx_i}$
$P_{11}(1710)$	πN	17(5)	15(4)	+0.15(4)
1662(7)	ηN	13(7)	11(7)	−0.13(4)
116(17)	$K\Lambda$	10(6)	8(4)	−0.11(3)
	$(\pi\Delta)_P$	7(4)	6(3)	−0.09(2)
	$\rho_1 N$	20(7)	17(6)	−0.16(2)
	σN	<1	<1	−0.00(2)
$P_{13}(1720)$	πN	27(3)	13.6(6)	+0.136(6)
1720(5)	ηN	<1	<1	+0.00(2)
200(20)	$K\Lambda$	6(1)	2.8(4)	−0.061(5)
	$\rho_1 N$	3(1)	1.4(5)	+0.04(1)
$F_{15}(1860)$	πN	37(3)	17(1)	+0.17(1)
1900(7)	ηN	9(4)	4(2)	−0.08(2)
219(23)	$K\Lambda$	0.8(4)	<1	−0.02(1)
	$(\pi\Delta)_P$	<4	<2	−0.03(3)
	$(\pi\Delta)_F$	<1	<1	+0.00(2)
	$(\rho_3 N)_P$	7(5)	3(2)	−0.07(3)
	σN	89(15)	41(6)	+0.26(2)
$D_{13}(1875)$	πN	36(12)	7(2)	+0.07(2)
1951(27)	$(\pi\Delta)_S$	434(39)	87(3)	−0.25(4)
500(45)	$(\pi\Delta)_D$	<28	<6	−0.04(2)
	$(\rho_3 N)_S$	<24	<5	+0.04(2)
	σN	<19	<4	+0.03(3)
$P_{11}(1880)$	πN	74(25)	15(5)	+0.15(5)
1900(36)	ηN	80(42)	16(7)	+0.16(4)
485(142)	$K\Lambda$	157(61)	32(10)	+0.22(3)
	$(\pi\Delta)_P$	<9	<2	−0.03(3)
	$\rho_1 N$	<2	<1	+0.01(4)
	σN	40(24)	8(5)	+0.11(3)
$S_{11}(1895)$	πN	85(11)	17(2)	+0.17(2)
1910(15)	ηN	203(29)	40(4)	+0.26(2)
502(47)	$K\Lambda$	9(5)	1.8(8)	+0.06(1)
	$(\pi\Delta)_D$	37(15)	7(3)	+0.11(2)
	$(\rho_3 N)_D$	43(12)	9(3)	−0.12(2)
	$\rho_1 N$	<9	<2	+0.04(2)
	σN	<6	<2	+0.03(2)
	πN^*	118(25)	24(4)	−0.20(2)
$P_{13}(1900)$	πN	7(4)	7(4)	+0.07(4)
1900(8)	ηN	<1	<1	+0.00(2)
101(15)	$K\Lambda$	14(5)	14(5)	−0.10(4)
	$\rho_1 N$	64(9)	64(7)	+0.21(8)
$G_{17}(2190)$	πN	101(18)	20(1)	+0.20(1)
2150(26)	ηN	9(7)	2(1)	−0.06(2)
500(74)	$K\Lambda$	<1	<1	+0.01(1)
	$(\rho_3 N)_D$	45(33)	9(6)	−0.13(5)

TABLE II. Resonance parameters for states with isospin $I = 3/2$. (See caption to Table I for details.)

Resonance	Channel	Γ_i (MeV)	$\mathcal{B}_i$ (%)	$\sqrt{xx_i}$	Resonance	Channel	Γ_i (MeV)	$\mathcal{B}_i$ (%)	$\sqrt{xx_i}$
$P_{33}(1232)$	πN	112.4(5)	99.4	+0.994	$P_{31}(1910)$	πN	36(2)	17(1)	+0.17(1)
1231.1(2)	$(\pi\Delta)_P$	0	0	+0.00	1934(5)	πN^*	99(14)	47(6)	−0.28(2)
113.0(5)	πN^*	0	0	+0.00	211(11)				
$P_{33}(1600)$	πN	18(4)	8(2)	+0.08(2)	$P_{33}(1920)$	πN	63(19)	16(4)	+0.16(4)
1626(8)	$(\pi\Delta)_P$	157(11)	70(3)	+0.24(2)	2146(32)	$(\pi\Delta)_P$	27(21)	7(5)	−0.10(4)
225(18)	πN^*	49(9)	22(3)	+0.13(1)	400(80)	πN^*	<83	<20	+0.12(7)
$S_{31}(1620)$	πN	37(2)	33(2)	+0.33(2)	$D_{35}(1930)$	πN	19(5)	7.9(4)	+0.079(4)
1600(1)	$(\pi\Delta)_D$	35(2)	32(2)	−0.32(1)	1930(12)				
112(2)	$(\rho_3 N)_D$	<1	<1	−0.03(1)	235(39)				
	$\rho_1 N$	29(2)	26(2)	+0.29(1)					
	πN^*	10(1)	9(1)	−0.17(1)					
$D_{33}(1700)$	πN	36(2)	14(1)	+0.14(1)	$F_{37}(1950)$	πN	118(2)	45.6(4)	+0.456(4)
1691(4)	$(\pi\Delta)_S$	134(6)	54(3)	+0.28(1)	1918(1)	$(\pi\Delta)_F$	22(3)	8(1)	+0.20(1)
248(9)	$(\pi\Delta)_D$	4(2)	1(1)	+0.05(2)	259(4)				
	$(\rho_3 N)_S$	75(7)	30(3)	+0.21(1)					
$S_{31}(1900)$	πN	20(4)	8(1)	+0.08(1)	$F_{35}(2000)$	πN	34(6)	7(1)	+0.07(1)
1868(12)	$(\pi\Delta)_D$	132(18)	56(6)	−0.22(2)	2015(24)	$(\pi\Delta)_P$	13(13)	3(3)	−0.04(2)
234(27)	$(\rho_3 N)_D$	53(15)	23(5)	−0.14(2)	500(52)	$(\pi\Delta)_F$	<13	<3	+0.02(3)
	$\rho_1 N$	29(10)	12(4)	−0.10(2)		$(\rho_3 N)_P$	449(49)	90(3)	+0.25(1)
	πN^*	<2	<1	+0.01(2)					
$F_{35}(1905)$	πN	16(2)	6(1)	+0.06(1)					
1818(8)	$(\pi\Delta)_P$	77(19)	28(7)	+0.13(2)					
278(18)	$(\pi\Delta)_F$	177(27)	64(8)	+0.19(2)					
	$(\rho_3 N)_P$	<14	<6	−0.04(2)					

With these, the total T matrix takes the form

$$T = B^T T_R B + T_B. \tag{3}$$

To obtain the elements of T_R, a resonant K matrix is constructed such that

$$T_R = K(I - iK)^{-1}. \tag{4}$$

The elements of the resonant K matrix are of the form

$$K_{ij} = \sum_{\alpha=1}^{N} X_{i\alpha} X_{j\alpha} \tan\delta_\alpha, \tag{5}$$

where α denotes a specific resonance and N is the number of resonances in the energy range of the fit; δ_α is an energy-dependent phase and $X_{i\alpha}$ is related to the branching ratio for resonance α to decay into channel i, and for each resonance, $\sum_i (X_{i\alpha})^2 = 1$. If $N = 1$, then $\tan\delta = (\Gamma/2)/(M - W)$ and $X_i^2 = \Gamma_i/\Gamma$, where Γ_i is the partial width for the ith channel. The corresponding K- and T_R-matrix elements are $K_{ij} = X_i \cdot X_j(\Gamma/2)/(M - W)$ and

$$[T_R]_{ij} = X_i \cdot X_j \frac{\Gamma/2}{M - W - \mathrm{i}\Gamma/2}, \tag{6}$$

respectively. For the special case of two resonances, $K_{ij} = X_{i1} \cdot X_{j1} \tan\alpha_1 + X_{i2} \cdot X_{j2} \tan\alpha_2$, so that

$$\begin{aligned}[T_R]_{ij} = {} & (X_{i1} \cdot X_{j1})C_{11} + (X_{i1} \cdot X_{j2})C_{12} \\ & + (X_{i2} \cdot X_{j1})C_{21} + (X_{i2} \cdot X_{j2})C_{22},\end{aligned} \tag{7}$$

where the energy-dependent coefficients C_{ij} can be calculated analytically [16]. Generalizing to N resonances, we can write

$$[T_R]_{ij} = \sum_{\alpha=1}^{N} \sum_{\beta=1}^{N} X_{i\alpha} [D^{-1}]_{\alpha\beta} X_{j\beta}. \tag{8}$$

The energy dependence of the phases δ_α is determined in a nontrivial and novel way such that

$$[D^{-1}]_{\alpha\beta} \propto \prod_{\gamma=1}^{N} [M_\gamma - W - \mathrm{i}(\Gamma_\gamma/2)]^{-1}, \tag{9}$$

where M_γ is a constant and W is the total c.m. energy. M_γ and Γ_γ evaluated at $W = M_\gamma$ represent conventional Breit-Wigner parameters. Each of the resonances corresponds to a pole in T_R and, therefore, also in the total S matrix. The poles occur at complex energies $W = W_\gamma$, where $M_\gamma - W_\gamma - \mathrm{i}(\Gamma_\gamma/2) = 0$.

III. FITTING PROCEDURE

The amplitudes for the multichannel energy-dependent fit were obtained from various single-energy analyses. Our energy-dependent fit included the SAID SP06 solution for $\pi N \to \pi N$ [12], the SAID FA07 solution for $\gamma N \to \pi N$ [22], and the solution of Manley *et al.* [23] for $\pi N \to \pi\pi N$. In some of the photoproduction amplitudes there were no single-energy solutions above 1.8 GeV. In such cases we used an average of the SAID current solution and the SAID SM95 solution [24]. In addition, we included our single-energy amplitudes for $\pi N \to \eta N$ and $\pi N \to K\Lambda$ [14]. Previous

TABLE III. Comparison of resonance parameters for $I = 1/2$ states with other analyses.

Mass (MeV)	Width (MeV)	Elasticity	Analysis	Mass (MeV)	Width (MeV)	Elasticity	Analysis
	$S_{11}(1535)$ ****				$D_{13}(1700)$ ***		
1538(1)	141(4)	0.37(1)	This work	1665(3)	56(8)	0.028(5)	This work
1519(5)	128(14)	0.54(5)	Anisovich 12 [32]	1790(40)	390(140)	0.12(5)	Anisovich 12 [32]
1547.0(7)	188.4(38)	0.355(2)	Arndt 06 [12]	1737(44)	250(220)	0.01(2)	Manley 92 [18]
1534(7)	151(27)	0.51(5)	Manley 92 [18]	1675(25)	90(40)	0.11(5)	Cutkosky 80 [8]
1550(40)	240(80)	0.50(10)	Cutkosky 80 [8]	1731(15)	110(30)	0.08(3)	Höhler 79 [28]
1526(7)	120(20)	0.38(4)	Höhler 79 [28]				
	$S_{11}(1650)$ ****				$D_{13}(1875)$ ***		
1664(2)	126(3)	0.57(2)	This work	1951(27)	500(45)	0.07(2)	This work
1651(6)	104(10)	0.51(4)	Anisovich 12 [32]	1880(20)	200(25)	0.03(2)	Anisovich 12 [32]
1634.7(11)	115.4(28)	1.0	Arndt 06 [12]	1804(55)	450(185)	0.23(3)	Manley 92 [18]
1659(9)	173(12)	0.89(10)	Manley 92 [18]	1880(100)	180(60)	0.10(4)	Cutkosky 80 [8]
1650(30)	150(40)	0.65(10)	Cutkosky 80 [8]	2060(80)	300(100)	0.14(7)	Cutkosky 80 [8]
1670(8)	180(20)	0.61(4)	Höhler 79 [28]	2081(20)	265(40)	0.06(2)	Höhler 79 [28]
	$S_{11}(1895)$ **				$D_{15}(1675)$ ****		
1910(15)	502(47)	0.17(2)	This work	1679(1)	145(4)	0.386(6)	This work
1895(15)	90^{+30}_{-15}	0.02(1)	Anisovich 12 [32]	1664(5)	152(7)	0.40(3)	Anisovich 12 [32]
1928(59)	414(157)	0.10(10)	Manley 92 [18]	1674.1(2)	146.5(10)	0.393(1)	Arndt 06 [12]
2180(80)	350(100)	0.18(8)	Cutkosky 80 [8]	1676(2)	159(7)	0.47(2)	Manley 92 [18]
1880(20)	95(30)	0.09(5)	Höhler 79 [28]	1675(10)	160(20)	0.38(5)	Cutkosky 80 [8]
				1679(8)	120(15)	0.38(3)	Höhler 79 [28]
	$P_{11}(1440)$ ****				$D_{15}(2060)$ **		
1412(2)	248(5)	0.648(9)	This work	2116(21)	307(112)	0.09(2)	This work
1430(8)	365(35)	0.62(3)	Anisovich 12 [32]	2060(15)	375(25)	0.08(2)	Anisovich 12 [32]
1485.0(12)	284(18)	0.787(16)	Arndt 06 [12]	2180(80)	400(100)	0.10(3)	Cutkosky 80 [8]
1462(10)	391(34)	0.69(3)	Manley 92 [18]	2228(30)	310(50)	0.07(2)	Höhler 79 [28]
1440(30)	340(70)	0.68(4)	Cutkosky 80 [8]				
1410(12)	135(10)	0.51(5)	Höhler 79 [28]				
	$P_{11}(1710)$ ***				$F_{15}(1680)$ ****		
1662(7)	116(17)	0.15(4)	This work	1682.7(5)	126(1)	0.680(5)	This work
1710(20)	200(18)	0.05(4)	Anisovich 12 [32]	1689(6)	118(6)	0.64(5)	Anisovich 12 [32]
1717(28)	480(230)	0.09(4)	Manley 92 [18]	1680.1(2)	128.0(11)	0.701(1)	Arndt 06 [12]
1650(30)	150(40)	0.65(10)	Cutkosky 80 [8]	1684(4)	139(8)	0.70(3)	Manley 92 [18]
1670(8)	180(20)	0.61(4)	Höhler 79 [28]	1680(10)	120(10)	0.62(5)	Cutkosky 80 [8]
				1684(3)	128(8)	0.65(2)	Höhler 79 [28]
	$P_{11}(1880)$ **				$F_{15}(1860)$ **		
1900(36)	485(142)	0.15(5)	This work	1900(7)	219(23)	0.17(1)	This work
1870(35)	235(65)	0.05(3)	Anisovich 12 [32]	1860^{+120}_{-60}	270^{+140}_{-50}	0.20(6)	Anisovich 12 [32]
1885(30)	113(44)	0.15(6)	Manley 92 [18]	1817.7	117.6	0.127	Arndt 06 [12]
				1903(87)	490(310)	0.08(5)	Manley 92 [18]
				1882(10)	95(20)	0.04(2)	Höhler 79 [28]
	$P_{13}(1720)$ ****				$F_{17}(1990)$ **		
1720(5)	200(20)	0.136(6)	This work	1990(45)	203(161)	0.02(1)	This work
1690^{+70}_{-35}	420(100)	0.10(5)	Anisovich 12 [32]	2060(65)	240(50)	0.02(1)	Anisovich 12 [32]
1763.8(46)	210(22)	0.094(5)	Arndt 06 [12]	2086(28)	535(120)	0.06(2)	Manley 92 [18]
1717(31)	380(180)	0.13(5)	Manley 92 [18]	1970(50)	350(120)	0.06(2)	Cutkosky 80 [8]
1700(50)	125(70)	0.10(5)	Cutkosky 80 [8]	2005(150)	350(100)	0.04(2)	Höhler 79 [28]
1710(20)	190(30)	0.14(3)	Höhler 79 [28]				
	$P_{13}(1900)$ ***				$G_{17}(2190)$ ****		
1900(8)	101(15)	0.07(4)	This work	2150(26)	500(74)	0.20(1)	This work
1905(30)	250^{+120}_{-50}	0.03(2)	Anisovich 12 [32]	2180(20)	335(40)	0.16(2)	Anisovich 12 [32]
1879(17)	498 (78)	0.26(6)	Manley 92 [18]	2152.4(14)	484(13)	0.22(1)	Arndt 06 [12]
				2127(9)	550(50)	0.70(3)	Manley 92 [18]
				2200(70)	500(150)	0.12(6)	Cutkosky 80 [8]
				2140(12)	390(90)	0.14(2)	Höhler 79 [28]

TABLE III. (*Continued.*)

Mass (MeV)	Width (MeV)	Elasticity	Analysis	Mass (MeV)	Width (MeV)	Elasticity	Analysis
	$D_{13}(1520)$ ****						
1512.6(5)	117(1)	0.627(5)	This work				
1517(3)	114(5)	0.62(3)	Anisovich 12 [32]				
1514.5(2)	103.6(4)	0.632(1)	Arndt 06 [12]				
1524(4)	124(8)	0.59(3)	Manley 92 [18]				
1525(10)	120(15)	0.58(3)	Cutkosky 80 [8]				
1519(4)	114(7)	0.54(3)	Höhler 79 [28]				

TABLE IV. Comparison of resonance parameters for $I = 3/2$ states with other analyses.

Mass (MeV)	Width (MeV)	Elasticity	Analysis	Mass (MeV)	Width (MeV)	Elasticity	Analysis
	$P_{33}(1232)$ ****				$S_{31}(1900)$ **		
1231.1(2)	113.0(5)	0.99	This work	1868(12)	234(27)	0.08(1)	This work
1228(2)	110(3)	1.0	Anisovich 12 [32]	1840(30)	300(45)	0.07(3)	Anisovich 12 [32]
1233.4(4)	118.7(6)	1.0	Arndt 06 [12]	1920(24)	263(39)	0.41(4)	Manley 92 [18]
1231(1)	118(4)	1.0	Manley 92 [18]	1890(50)	170(50)	0.10(3)	Cutkosky 80 [8]
1232(3)	120(5)	1.0	Cutkosky 80 [8]	1908(30)	140(40)	0.08(4)	Höhler 79 [28]
1233(2)	116(5)	1.0	Höhler 79 [28]				
	$P_{33}(1600)$ ***				$F_{35}(1905)$ ****		
1626(8)	225(18)	0.08(2)	This work	1818(8)	278(18)	0.06(1)	This work
1510(20)	220(45)	0.12(5)	Anisovich 12 [32]	1861(6)	335(18)	0.13(2)	Anisovich 12 [32]
1706(10)	430(73)	0.12(2)	Manley 92 [18]	1857.8(16)	320.6(86)	0.122(1)	Arndt 06 [12]
1600(50)	300(100)	0.18(4)	Cutkosky 80 [8]	1881(18)	327(51)	0.12(3)	Manley 92 [18]
1522(13)	220(40)	0.21(6)	Höhler 79 [28]	1910(30)	400(100)	0.08(3)	Cutkosky 80 [8]
				1905(20)	260(20)	0.15(2)	Höhler 79 [28]
	$S_{31}(1620)$ ****				$P_{31}(1910)$ ****		
1600(1)	112(2)	0.33(2)	This work	1934(5)	211(11)	0.17(1)	This work
1600(8)	130(11)	0.28(3)	Anisovich 12 [32]	1860(40)	350(55)	0.12(3)	Anisovich 12 [32]
1615.2(4)	146.9(19)	0.315(1)	Arndt 06 [12]	2067.9(17)	543(10)	0.239(1)	Arndt 06 [12]
1672(7)	154(37)	0.09(2)	Manley 92 [18]	1882(10)	239(25)	0.23(8)	Manley 92 [18]
1620(20)	140(20)	0.25(3)	Cutkosky 80 [8]	1910(40)	225(50)	0.19(3)	Cutkosky 80 [8]
1610(7)	139(18)	0.35(6)	Höhler 79 [28]	1888(20)	280(50)	0.24(6)	Höhler 79 [28]
	$D_{33}(1700)$ ****				$P_{33}(1920)$ ***		
1691(4)	248(9)	0.14(1)	This work	2146(32)	400(80)	0.16(4)	This work
1715^{+30}_{-15}	310^{+40}_{-15}	0.22(4)	Anisovich 12 [32]	1900(30)	310(60)	0.08(4)	Anisovich 12 [32]
1695.0(13)	375.5(70)	0.156(1)	Arndt 06 [12]	2014(16)	152(55)	0.02(2)	Manley 92 [18]
1762(44)	600(250)	0.14(6)	Manley 92 [18]	1920(80)	300(100)	0.20(5)	Cutkosky 80 [8]
1710(30)	280(80)	0.12(3)	Cutkosky 80 [8]	1868(80)	220(80)	0.14(4)	Höhler 79 [28]
1680(70)	230(80)	0.20(3)	Höhler 79 [28]				
	$D_{35}(1930)$ ***				$F_{35}(2000)$ **		
1930(12)	235(39)	0.079(4)	This work	2015(24)	500(52)	0.07(1)	This work
2233(53)	773(187)	0.081(12)	Arndt 06 [12]	1752(32)	251(93)	0.02(1)	Manley 92 [18]
1956(22)	530(140)	0.18(2)	Manley 92 [18]	2200(125)	400(125)	0.07(4)	Cutkosky 80 [8]
1940(30)	320(60)	0.14(4)	Cutkosky 80 [8]	1724(61)	138(68)	0.00(1)	Vrana 00 [26]
1901(15)	195(60)	0.04(3)	Höhler 79 [28]				
	$F_{37}(1950)$ ****						
1918(1)	259(4)	0.456(4)	This work				
1915(6)	246(10)	0.45(2)	Anisovich 12 [32]				
1921.3(2)	271.1(11)	0.471(1)	Arndt 06 [12]				
1945(2)	300(7)	0.38(1)	Manley 92 [18]				
1950(15)	340(50)	0.39(4)	Cutkosky 80 [8]				
1913(8)	224(10)	0.38(2)	Höhler 79 [28]				

TABLE V. Comparison of pole positions (in MeV) for $I = 1/2$ states with other analyses.

Resonance	Real part	$-2\times$Imaginary part	Analysis	Resonance	Real part	$-2\times$Imaginary part	Analysis
$P_{11}(1440)$	1370	214	This work	$F_{15}(1860)$	1863	189	This work
****	1370(4)	190(7)	Anisovich 12 [32]	**	1830^{+120}_{-60}	250^{+150}_{-50}	Anisovich 12 [32]
	1359	162	Arndt 06 [12]		1807	109	Arndt 06 [12]
	1385	164	Höhler 93 [31]				
	1375(30)	180(40)	Cutkosky 80 [8]				
$D_{13}(1520)$	1501	112	This work	$D_{13}(1875)$	1975	495	This work
****	1507(3)	111(5)	Anisovich 12 [32]	**	1860(25)	200(20)	Anisovich 12 [32]
	1515	113	Arndt 06 [12]		1880(100)	160(80)	Cutkosky 80 [8]
	1510	120	Höhler 93 [31]				
	1510(5)	114(10)	Cutkosky 80 [8]				
$S_{11}(1535)$	1515	123	This work	$P_{11}(1880)$	1801	383	This work
****	1501(4)	134(11)	Anisovich 12 [32]	**	1860(35)	250(70)	Anisovich 12 [32]
	1502	95	Arndt 06 [12]				
	1487	–	Höhler 93 [31]				
	1510(10)	260(80)	Cutkosky 80 [8]				
$S_{11}(1650)$	1655	123	This work	$S_{11}(1895)$	1858	479	This work
****	1647(6)	103(8)	Anisovich 12 [32]	**	1900(15)	90^{+30}_{-15}	Anisovich 12 [32]
	1648	80	Arndt 06 [12]		2150(70)	350(100)	Cutkosky 80 [8]
	1670	163	Höhler 93 [31]		1937 or 1949	139 or 131	Longacre 78 [33]
	1640(20)	150(30)	Cutkosky 80 [8]				
$D_{15}(1675)$	1656	128	This work	$P_{13}(1900)$	1895	100	This work
****	1654(4)	151(5)	Anisovich 12 [32]	**	1900(30)	200^{+100}_{-60}	Anisovich 12 [32]
	1657	139	Arndt 06 [12]				
	1656	126	Höhler 93 [31]				
	1660(10)	140(10)	Cutkosky 80 [8]				
$F_{15}(1680)$	1669	119	This work	$F_{17}(1990)$	1941	130	This work
****	1676(6)	113(4)	Anisovich 12 [32]	**	2030(65)	240(60)	Anisovich 12 [32]
	1674	115	Arndt 06 [12]		1900(30)	260(60)	Cutkosky 80 [8]
	1673	135	Höhler 93 [31]				
	1667(5)	110(10)	Cutkosky 80 [8]				
$D_{13}(1700)$	1662	55	This work	$D_{15}(2060)$	2064	267	This work
***	1770(40)	420(180)	Anisovich 12 [32]	**	2040(15)	390(25)	Anisovich 12 [32]
	1700	120	Höhler 93 [31]		2100(60)	360(80)	Cutkosky 80 [8]
	1660(30)	90(40)	Cutkosky 80 [8]				
$P_{11}(1710)$	1644	104	This work	$G_{17}(2190)$	2062	428	This work
***	1687(17)	200(25)	Anisovich 12 [32]	****	2150(25)	330(30)	Anisovich 12 [32]
	1690	200	Höhler 93 [31]		2070	520	Arndt 06 [12]
	1698	88	Cutkosky 90 [30]		2042	482	Höhler 93 [31]
	1690(20)	80(20)	Cutkosky 80 [8]		2100(50)	400(160)	Cutkosky 80 [8]
$P_{13}(1720)$	1687	175	This work				
****	1660(30)	450(100)	Anisovich 12 [32]				
	1666	355	Arndt 06 [12]				
	1686	187	Höhler 93 [31]				
	1680(30)	120(40)	Cutkosky 80 [8]				

single-channel analyses [25–27] of $\pi N \to \eta N$ and $\pi N \to K\Lambda$ were simplistic energy-dependent PWAs that failed to satisfy S-matrix unitarity. A multichannel energy-dependent fit was performed in the c.m. energy range from 1080 to 2100 MeV. Initially some approximately known fitting parameters were held fixed to yield a good fit. In some partial waves, ωN and $\rho\Delta$ channels were included as dummy channels (channels without data) to satisfy unitarity. In our final fits, uncertainties in resonance parameters were calculated with all fitting parameters free to vary.

IV. DISCUSSION OF RESONANCE PARAMETERS

The hadronic resonance parameters for states with $I = 1/2$ and $I = 3/2$ are listed in Tables I and II, respectively. The first column lists the resonance name together with the fitted resonance mass and its fitted total width in MeV. The second column lists the fitted hadronic decay channels, starting with πN elastic channel. Quasi-two-body $\pi\pi N$ channels are tabulated as $\pi\Delta$, ρN, σN, or πN^*, where σ denotes the s-wave $\pi\pi$ system with $J^P = 0^+$ and $I_{\pi\pi} = 0$, and N^* denotes the $P_{11}(1440)$ resonance. Sometimes a subscript appears with a channel notation [e.g.. $(\pi\Delta)_D$]; here the subscript denotes the orbital angular momentum of the channel. Also a subscript after the meson symbol in a reaction channel (e.g., $\rho_3 N$) refers to twice the sum of the intrinsic spins ($2S$) of the meson and baryon. The third column in Table I or II lists the partial decay widths (Γ_i) associated with corresponding channels. The symbol $\mathcal{B}_i$ in the fourth column denotes the branching ratio for a given channel. Finally, the x and x_i represent the ratio of elastic partial width and partial width for the ith channel respectively to the total width.

In Tables III and IV we compare our results on resonance parameters (resonance mass, width, and elasticity) for $I = 1/2$ and $I = 3/2$ states with prior analyses. Any resonance included above 2.1 GeV had its mass parameter initially fixed and resonance parameters for these states are generally not listed. For most resonances, the PDG star rating [6] is included in column 1.

In Tables V and VI we list the complex pole positions of resonances and compare our results with prior analyses. Here, the first column lists the name of the resonance, the second column lists the real part of the pole position (pole mass), and the third column lists the pole width, which is given by the negative of twice the imaginary part of the pole position.

Figures 1–5 show representative Argand diagrams for the elastic and two inelastic ($\pi N \to \eta N$ and $\pi N \to K\Lambda$) amplitudes for $I = 1/2$ partial waves (for D_{13} only elastic amplitude is shown) and representative Argand diagrams for the elastic $I = 3/2$ amplitudes. To discuss the resonance parameters we follow a logical sequence of partial waves.

$\mathbf{S_{11}}$: This partial wave was fitted with three resonances. The first resonance occurred with a mass M = 1538 ± 1 MeV and width Γ = 141 ± 4 MeV and corresponds to the 4* $S_{11}(1535)$. The strength of this resonance divides more or less equally to πN and ηN at 37% and 41%, respectively, with the remainder going to $\pi\pi N$ channels. Our results for this state agree quite well with those from previous analyses, especially Ref. [28]. The second resonance was seen to have M = 1664 ± 2 MeV and Γ = 126 ± 3 MeV corresponding to the 4* $S_{11}(1650)$. Decay modes for this state are primarily πN, ηN, $K\Lambda$, $\pi\Delta$, and $\rho_1 N$. We found the third resonance with M = 1910 ± 15 MeV and Γ = 502 ± 47 MeV corresponding to the 2* $S_{11}(1895)$. There is striking resemblance of our ηN amplitude for the partial wave S_{11} with one solution presented by Batinić *et al.* [29].

For $S_{11}(1535)$, our pole mass M_p = 1515 MeV and pole width Γ_p = 123 MeV are in good agreement with previous

TABLE VI. Comparison of pole positions (in MeV) for $I = 3/2$ states with other analyses.

Resonance	Real part	−2×Imaginary part	Analysis	Resonance	Real part	−2×Imaginary part	Analysis
$P_{33}(1232)$	1212	98	This work	$F_{35}(1905)$	1769	239	This work
****	1210.5(10)	99(2)	Anisovich 12 [32]	****	1805(10)	300(15)	Anisovich 12 [32]
	1211	99	Arndt 06 [12]		1819	247	Arndt 06 [12]
	1209	100	Höhler 93 [31]		1829	303	Höhler 93 [31]
	1210(1)	100(2)	Cutkosky 80 [8]		1830(5)	280(60)	Cutkosky 80 [8]
	1211(1)	100(2)	Anisovich 10 [34]				
$P_{33}(1600)$	1599	211	This work	$P_{31}(1910)$	1910	199	This work
***	1498(25)	230(50)	Anisovich 12 [32]	****	1850(40)	350(45)	Anisovich 12 [32]
	1457	400	Arndt 06 [12]		1771	479	Arndt 06 [12]
	1550	–	Höhler 93 [31]		1874	283	Höhler 93 [31]
	1550(40)	200(60)	Cutkosky 80 [8]		1880(30)	200(40)	Cutkosky 80 [8]
$S_{31}(1620)$	1587	107	This work	$P_{33}(1920)$	2110	386	This work
****	1597(4)	130(9)	Anisovich 12 [32]	***	1890(30)	300(60)	Anisovich 12 [32]
	1595	135	Arndt 06 [12]		1900	–	Höhler 93 [31]
	1608	116	Höhler 93 [31]		1900(80)	300(100)	Cutkosky 80 [8]
	1600(15)	120(20)	Cutkosky 80 [8]				
	1596(7)	130(10)	Anisovich 10 [34]				
$D_{33}(1700)$	1656	226	This work	$D_{35}(1930)$	1882	187	This work
****	1680(10)	305(15)	Anisovich 12 [32]	***	2001	387	Arndt 06 [12]
	1632	253	Arndt 06 [12]		1850	180	Höhler 93 [31]
	1651	159	Höhler 93 [31]		1890(50)	260(60)	Cutkosky 80 [8]
	1675(25)	220(40)	Cutkosky 80 [8]				
	1650(30)	275(35)	Anisovich 10 [34]				
$S_{31}(1900)$	1844	223	This work	$F_{37}(1950)$	1871	220	This work
**	1845(25)	300(45)	Anisovich 12 [32]	****	1890(4)	243(8)	Anisovich 12 [32]
	1780	–	Höhler 93 [31]		1876	227	Arndt 06 [12]
	1870(40)	180(50)	Cutkosky 80 [8]		1878	230	Höhler 93 [31]
					1890(15)	260(40)	Cutkosky 80 [8]
				$F_{35}(2000)$	1976	488	This work
				**	2150(100)	350(100)	Cutkosky 80 [8]
					1697	112	Vrana 00 [26]

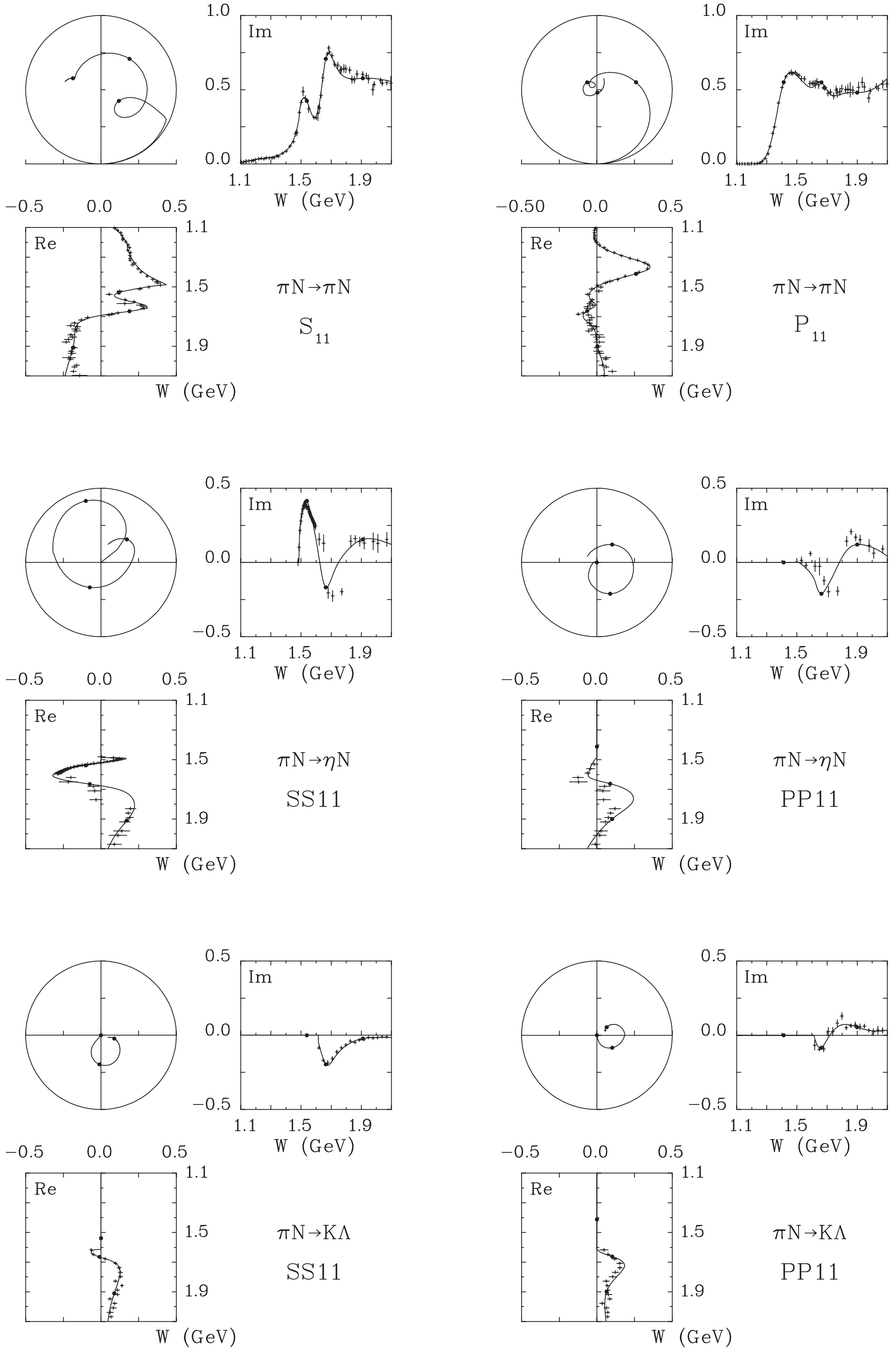

FIG. 1. Argand diagrams for two-body amplitudes.

analyses, especially that by Arndt *et al.* [12] and the same is true with the second resonance $S_{11}(1650)$ with $M_p = 1655$ MeV and $\Gamma_p = 123$ MeV. For the $S_{11}(1895)$, $M_p = 1858$ MeV and $\Gamma_p = 479$ MeV.

P_{11}: This partial wave was fitted with four resonances. The first resonance occurred at $M = 1412 \pm 2$ MeV with $\Gamma = 248 \pm 5$ MeV and corresponds to the 4* $P_{11}(1440)$. These results agree quite well with those from prior analyses, especially Ref. [8]. The decay modes are πN and $\pi\pi N$ channels. Our analysis confirms the existence of the state $P_{11}(1710)$, which is refuted or marked uncertain by the GWU analysis [12]. This resonance occurred at $M = 1662 \pm 7$ MeV

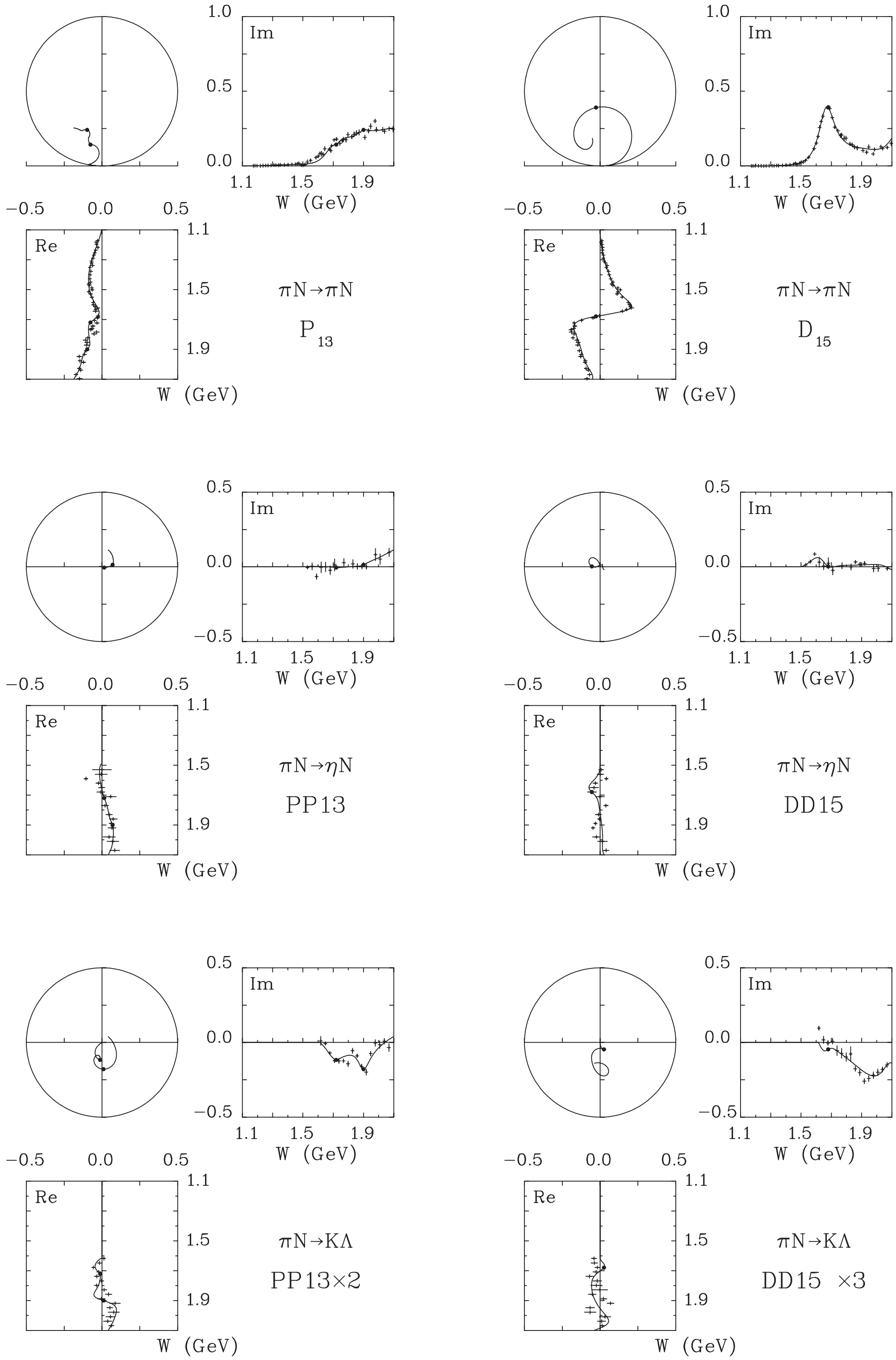

FIG. 2. Same as in Fig. 1.

with $\Gamma = 116 \pm 17$ MeV agreeing with the previous analysis by Cutkosky *et al.* [8]. Its elasticity is about 17%. The branching ratios for the ηN and KΛ channels are about 11% and 8%, respectively. The third resonance occurred at $M = 1900 \pm 36$ MeV with $\Gamma = 485 \pm 142$ MeV. This resonance corresponds to the 2* $P_{11}(1880)$. The major decay modes are πN, ηN, and $K\Lambda$. A fourth resonance was included at $M = 2250 \pm 116$ MeV and $\Gamma = 600 \pm 394$ MeV. During the fits, the mass of this resonance was held fixed but in the final zero-iteration fit we treated it as a free parameter.

For $P_{11}(1440)$, our pole mass $M_p = 1370$ MeV and pole width $\Gamma_p = 214$ MeV are in good agreement with prior

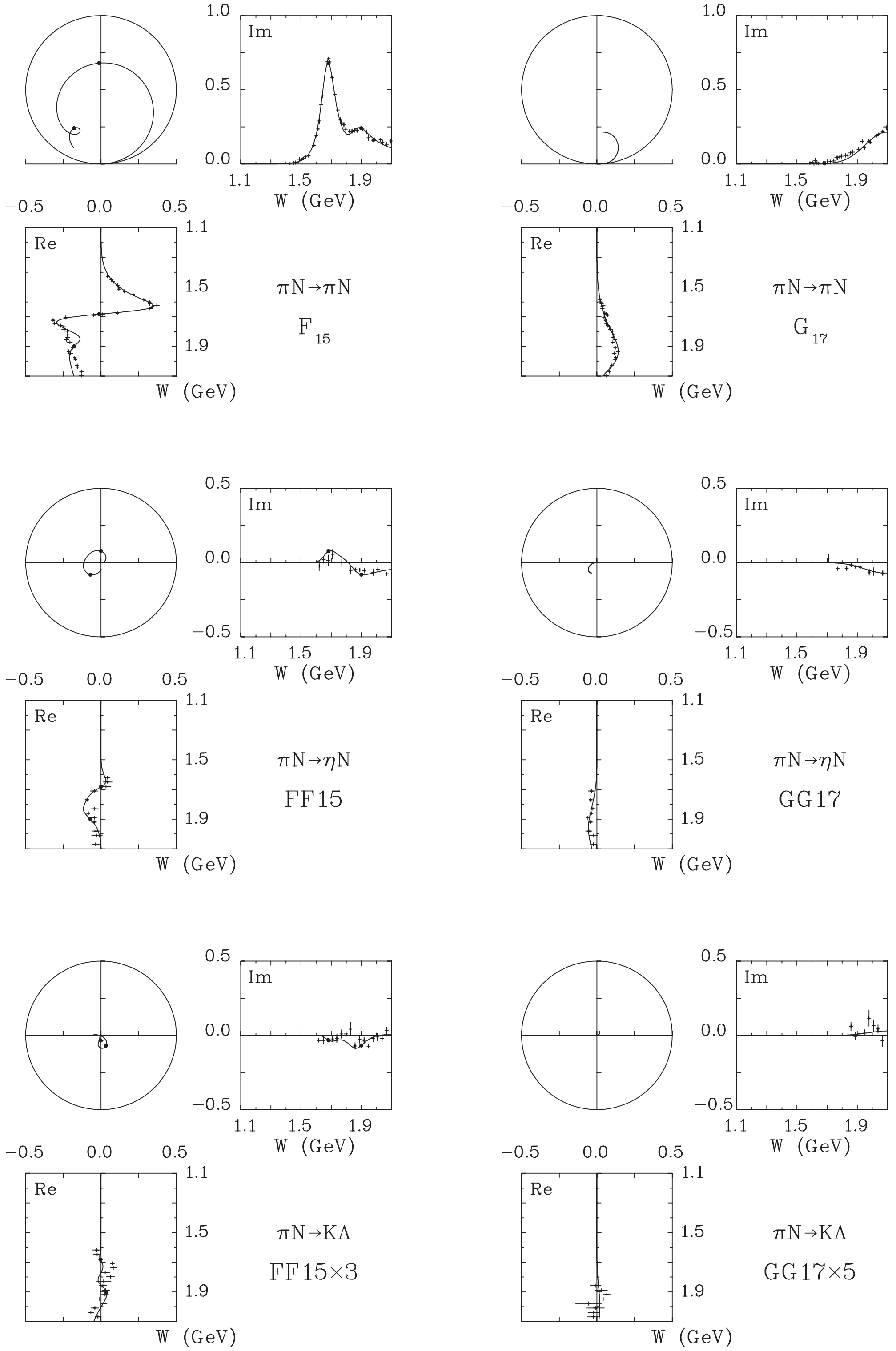

FIG. 3. Same as in Fig. 1.

analyses, especially that by Cutkosky *et al.* [8]. For $P_{11}(1710)$ our pole mass of $M_p = 1644$ MeV is slightly smaller than those given in previous analyses but the pole width $\Gamma_p = 104$ MeV is comparable with the results of Cutkosky and Wang [30] and Cutkosky *et al.* [8].

$\mathbf{P_{13}}$: This partial wave was fitted with two resonances. The first resonance occurred at $M = 1720 \pm 5$ MeV with $\Gamma = 200 \pm 20$ MeV and can be identified with the 4* $P_{13}(1720)$. Our results for this state agree very well with those from prior analyses, especially Ref. [28]. The major decay modes

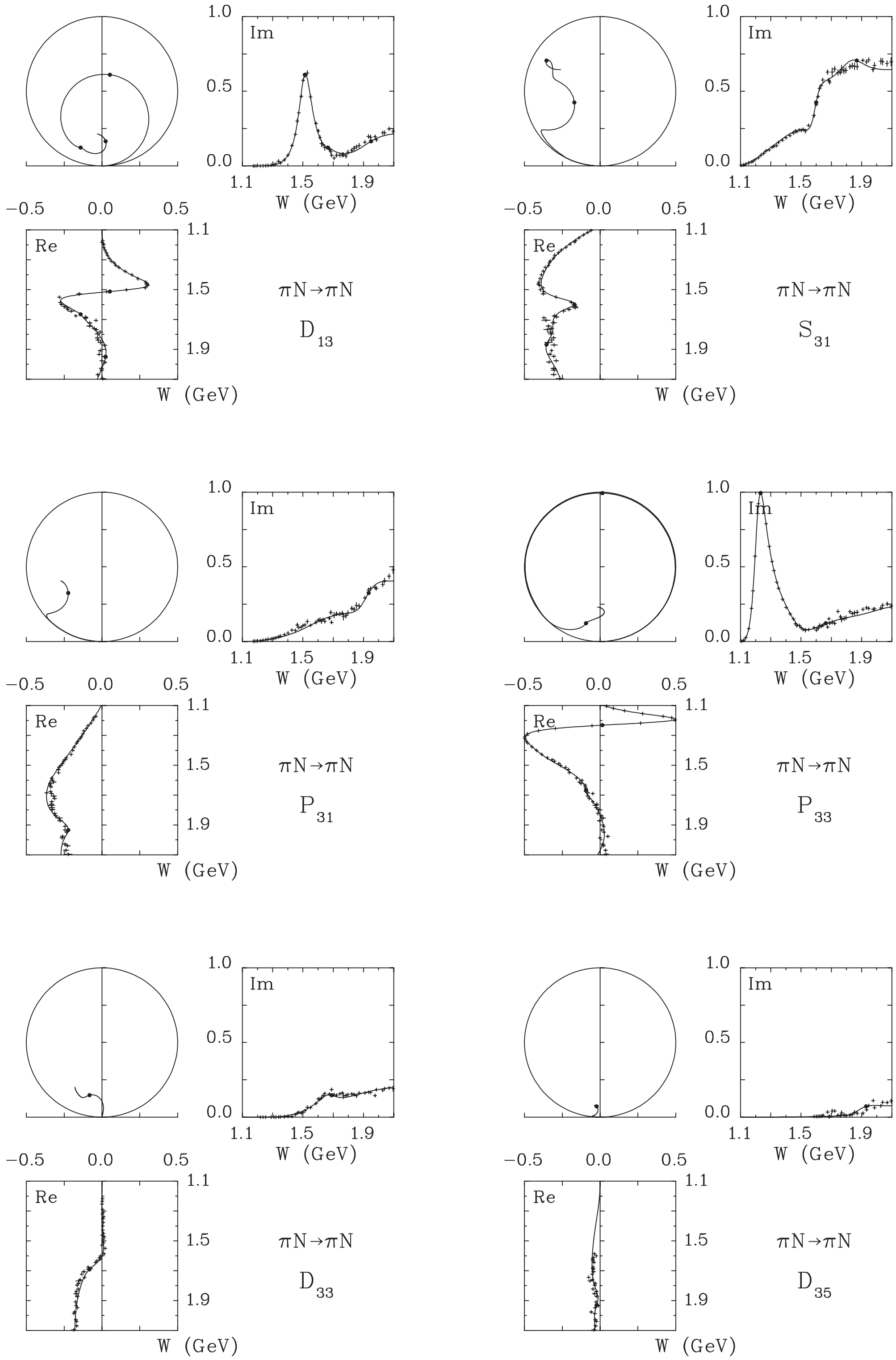

FIG. 4. Same as in Fig. 1.

were found to be πN (14%), $\rho_1 N$(1%), and $K\Lambda$ (3%). We found no coupling to the ηN channel. Most of the flux was seen to be carried by dummy $\rho\Delta$ and ωN channels. The second resonance corresponds to the 3* P_{13}(1900). The decay channels for this resonance were found to be πN (7%), $\rho_1 N$ (64%), and $K\Lambda$ (14%). Again no ηN coupling was seen.

For P_{13}(1720), the pole mass $M_p = 1687$ MeV and the pole width $\Gamma_p = 175$ MeV are in good agreement with previous analyses, especially that by Höhler [31].

D_{13}: This partial wave was fitted with four resonances. The first resonance occurred at $M = 1512.6 \pm 0.5$ MeV with $\Gamma = 117 \pm 1$ MeV, which corresponds to the 4* D_{13}(1520).

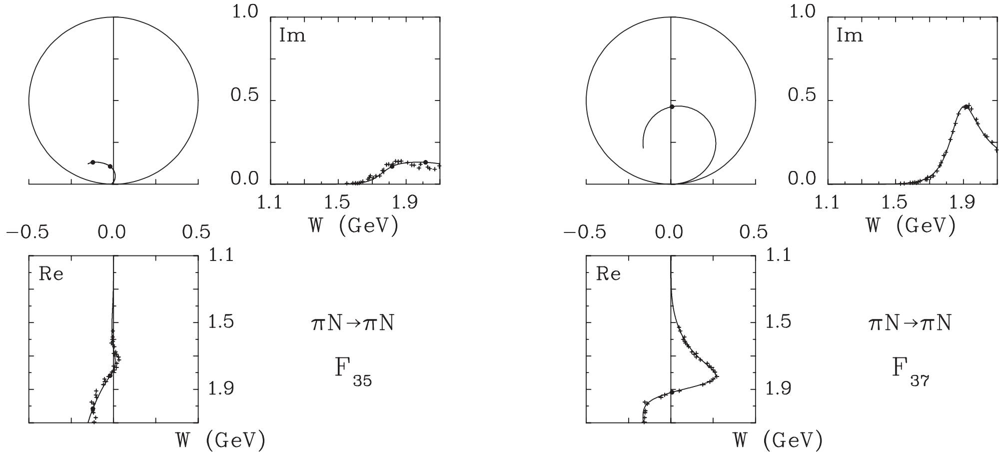

FIG. 5. Same as in Fig. 1.

Our results for this state agree very well with those from prior analyses. This state was seen to be highly elastic (63%) and other major decay modes were found to be $(\pi\Delta)_S$ (9%), $(\pi\Delta)_D$ (6%), and $\rho_3 N$ (21%). The second resonance occurred at $M = 1665 \pm 3$ MeV with $\Gamma = 56 \pm 8$ MeV. This state was found to be highly inelastic with major decay channels $(\pi\Delta)_S$ (31%), $\rho_3 N$ (38%), and σN (24%). The third resonance occurred at $M = 1951 \pm 27$ MeV with $\Gamma = 500 \pm 45$ MeV. Its major decay channel was $(\pi\Delta)_S$ (87%) and its elasticity was found to be about 7%. We didn't find any coupling to ηN and $K\Lambda$ channels with any of these excited states. The fourth resonance was included at $M = 2200 \pm 39$ MeV and $\Gamma = 750 \pm 101$ MeV.

For $D_{13}(1520)$, the pole mass $M_p = 1501$ MeV and the pole width $\Gamma_p = 112$ MeV are in very good agreement with previous analyses. For $D_{13}(1700)$, our pole mass $M_p = 1662$ MeV agrees quite well with the analysis by Cutkosky *et al.* [8] and our pole width of $\Gamma_p = 55$ MeV as well. For $D_{13}(1875)$ the pole mass of $M_p = 1975$ MeV agrees well with the previous analyses within uncertainties but our pole width $\Gamma_p = 495$ MeV is greater than those given in the prior analyses.

D$_{15}$: Two resonances were required to fit this partial wave. The first resonance occurred at $M = 1679 \pm 1$ MeV with $\Gamma = 145 \pm 4$ MeV. It corresponds to the 4* $D_{15}(1675)$. Our results for this state agree very well with those from previous analyses. The major decay channels were πN (39%), and $\pi\Delta$ (46%) with tiny couplings for ηN and $K\Lambda$. The second resonance was included at $M = 2116 \pm 21$ MeV with $\Gamma = 307 \pm 112$ MeV.

For $D_{15}(1675)$, the pole mass $M_p = 1656$ MeV and the pole width $\Gamma = 128$ MeV agree very well with previous analyses.

F$_{15}$: This partial wave was fitted with two resonances. The first resonance occurred at $M = 1682.7 \pm 0.5$ MeV with $\Gamma = 126 \pm 1$ MeV and can be identified with the 4* $F_{15}(1680)$. This resonance was found to be highly elastic with an elasticity of 68%. The elastic amplitude for this state exhibited classic Breit-Wigner behavior. The other hadronic channels were $(\pi\Delta)_P$ (11%), $(\pi\Delta)_F$ (1%), $(\rho_3 N)_P$ (7%), $(\rho_3 N)_F$ (2%), σN (9%), ηN (about 1%), and $K\Lambda$ (<1%). The second resonance occurred at $M = 1900 \pm 7$ MeV with $\Gamma = 219 \pm 23$ MeV and corresponds to the 2* $F_{15}(1860)$. In our initial fits we kept this mass fixed. This resulted in a small wiggle in the real part of the elastic amplitude near 1900 MeV, thereby disagreeing slightly with the GWU single-energy solution. The major decay modes were πN (17%), $(\rho_3 N)_F$ (34%), and σN (41%).

For $F_{15}(1680)$, the pole mass $M_p = 1669$ MeV and the pole width $\Gamma_p = 119$ MeV agree very well with previous analyses. For $F_{15}(1860)$, the pole mass $M_p = 1863$ MeV and pole width $\Gamma_p = 189$ MeV are slightly larger than those presented in the analysis by Arndt *et al.* [12].

F$_{17}$: This partial wave was fitted with a single resonance at $M = 1990 \pm 45$ MeV and $\Gamma = 203 \pm 161$ MeV. This resonance is highly inelastic with an elasticity of only 2%. The coupling to the $K\Lambda$ channel is also small with a branching ratio of <1%.

For $F_{17}(1990)$ the pole mass $M_p = 1941$ MeV agrees quite well with that by Cutkosky *et al.* [8] but our pole width $\Gamma_p = 130$ MeV is about half the value from that analysis.

G$_{17}$: This partial wave was fitted with one resonance at $M = 2150 \pm 26$ MeV with $\Gamma = 500 \pm 74$ MeV. This resonance corresponds to the 4* $G_{17}(2190)$. The decay channels were πN (20%), $(\rho_3 N)_D$ (9%), ηN (2%), and $K\Lambda$ (<1%), with most of the strength carried by a dummy ωN channel.

For $G_{17}(2190)$ the pole mass $M_p = 2062$ MeV and the pole width $\Gamma_p = 428$ MeV agree more or less with previous analyses.

S$_{31}$: Two resonances were required to fit this partial wave. The first resonance occurred at $M = 1600 \pm 1$ MeV with $\Gamma = 112 \pm 2$ MeV and can be identified with the 4* $S_{31}(1620)$. The primary decay modes for this state were found to be πN (33%), $(\pi\Delta)_D$ (32%), $\rho_1 N$ (26%), and πN^* (9%). The second resonance occurred at $M = 1868 \pm 12$ MeV with $\Gamma = 234 \pm 27$ MeV and corresponds to the 2* $S_{31}(1900)$. The major decay modes were found to be πN (8%), $\pi\Delta$ (56%), $\rho_3 N$ (23%), and πN^* (12%).

For $S_{31}(1620)$ the pole mass and width were found to be $M_p = 1587$ MeV and $\Gamma_p = 107$ MeV, respectively. Our pole width is comparable with that in previous analyses but our

TABLE VII. Comparison of helicity amplitudes (in 10^{-3} GeV$^{-1/2}$) for $I = 1/2$ and $I = 3/2$ states with other analyses.

$A^p_{\frac{1}{2}}$	$A^n_{\frac{1}{2}}$	$A^p_{\frac{3}{2}}$	$A^n_{\frac{3}{2}}$	Analysis	$A^p_{\frac{1}{2}}$	$A^n_{\frac{1}{2}}$	$A^p_{\frac{3}{2}}$	$A^n_{\frac{3}{2}}$	Analysis
		$P_{11}(1440)$ ****					$P_{11}(1710)$ ***		
−84(3)	40(5)			This work	−8(3)	17(3)			This work
−61(8)				Anisovich 12 [32]	52(15)				Anisovich 12 [32]
−51(2)				Dugger 07 [37]	7(15)	−2(15)			Arndt 96 [38]
−63(18)	45(15)			Arndt 96 [38]	6(18)				Crawford 83 [40]
					28(9)	0(18)			Awaji 81 [41]
		$D_{13}(1520)$ ****					$P_{13}(1720)$ ****		
−34(1)	−38(3)	127(3)	−101(4)	This work	57(3)	−2(1)	−19(2)	−1(2)	This work
−22(4)		131(10)		Anisovich 12 [32]	110(45)		150(30)		Anisovich 12 [32]
−28(2)		143(2)		Dugger 07 [37]	97(3)		−39(3)		Dugger 07 [37]
−38(3)		147(10)		Ahrens 02 [39]	−15(15)	7(15)	7(10)	−5(25)	Arndt 96 [38]
−20(7)	−48(8)	167(5)	−140(10)	Arndt 96 [38]	44(66)		−24(6)		Crawford 83 [40]
−28(14)		156(22)	−124(9)	Crawford 83 [40]	−4(7)	2(5)	−4(16)	−15(19)	Awaji 81 [41]
−7(4)	−66(13)	168(13)		Awaji 81 [41]					
		$S_{11}(1535)$ ****					$F_{15}(1860)$ **		
59(3)	−49(3)			This work	−17(3)	10(5)	29(4)	−9(5)	This work
105(10)				Anisovich 12 [32]	−19(11)		48(18)		Anisovich 12 [32]
90(25)	−80(20)			Anisovich 09 [35]					
91(2)				Dugger 07 [37]					
120(13)				Krusche 97 [42]					
60(15)	−20(35)			Arndt 96 [38]					
97(6)				Benmerrouch 95 [43]					
		$S_{11}(1650)$ ****					$D_{13}(1875)$ ***		
30(3)	11(2)			This work	7(8)	55(21)	43(22)	−85(31)	This work
33(7)				Anisovich 12 [32]	18(10)		−9(5)		Anisovich 12 [32]
100(35)	−55(20)			Anisovich 09 [35]	−20(8)	7(13)	17(11)	−53(34)	Awaji 81 [41]
22(7)				Dugger 07 [37]					
69(5)	−15(5)			Arndt 96 [38]					
		$D_{15}(1675)$ ****					$P_{11}(1880)$ **		
11(1)	−40(4)	20(1)	−68(4)	This work	21(6)	14(7)			This work
24(3)		25(7)		Anisovich 12 [32]	−13(3)				Anisovich 12a [32]
18(2)		21(1)		Dugger 07 [37]	34(11)				Anisovich 12b [32]
15(10)	−49(10)	10(7)	−51(10)	Arndt 96 [38]					
21(11)		15(9)		Crawford 83 [40]					
34(5)	−57(24)	24(8)	−77(18)	Awaji 81 [41]					
	−33(4)		−69(4)	Fujii 81 [44]					
		$F_{15}(1680)$ ****					$S_{11}(1895)$ **		
−17(1)	29(2)	136(1)	−59(2)	This work	12(6)	3(7)			This work
−13(3)		135(6)		Anisovich 12 [32]	−11(6)				Anisovich 12 [32]
−17(1)		134(2)		Dugger 07 [37]					
−10(4)	30(5)	145(5)	−40(15)	Arndt 96 [38]					
−17(18)		132(10)		Crawford 83 [40]					
−9(6)	17(14)	115(8)	−33(13)	Awaji 81 [41]					
	32(3)		−23(5)	Fujii 81 [44]					
		$D_{13}(1700)$ ***					$P_{13}(1900)$ ***		
21(5)	−49(8)	50(9)	−92(14)	This work	41(8)	−10(4)	−4(6)	−11(7)	This work
41(17)		−34(13)		Anisovich 12 [32]	26(15)		−65(30)		Anisovich 12 [32]
−16(14)		−9(12)		Crawford 83 [40]					
−2(13)	6(24)	29(14)	−33(17)	Awaji 81 [41]					
		$D_{15}(2060)$ **							
18(4)	−12(17)	10(4)	−23(23)	This work					
67(15)		55(20)		Anisovich 12 [32]					

TABLE VII. (*Continued.*)

$A^p_{\frac{1}{2}}$	$A^n_{\frac{1}{2}}$	$A^p_{\frac{3}{2}}$	$A^n_{\frac{3}{2}}$	Analysis	$A^p_{\frac{1}{2}}$	$A^n_{\frac{1}{2}}$	$A^p_{\frac{3}{2}}$	$A^n_{\frac{3}{2}}$	Analysis
		$P_{33}(1232)$ ****					$F_{35}(1905)$ ****		
−137(1)		−251(1)		This work	66(18)		−223(29)		This work
−131(4)		−254(5)		Anisovich 12 [32]	25(5)		−49(4)		Anisovich 12 [32]
−139(4)		−258(5)		Dugger 07 [37]	21(4)		−46(5)		Dugger 07 [37]
−141(5)		−261(5)		Arndt 96 [38]	22(5)		−45(5)		Arndt 96 [38]
−129(5)		−243(1)		Arndt 02 [45]	21(10)		−56(28)		Crawford 83 [40]
−145(15)		−263(26)		Crawford 83 [40]	43(20)		−25(23)		Awaji 81 [41]
−138(4)		−259(6)		Awaji 81 [41]					
		$P_{33}(1600)$ ***					$P_{31}(1910)$ ****		
6(5)		52(8)		This work	30(2)				This work
−50(9)		−40(12)		Anisovich 12 [32]	22(9)				Anisovich 12 [32]
−18(15)		−25(15)		Arndt 96 [38]	25(11)				Awaji 81 [41]
−39(30)		−13(14)		Crawford 83 [40]					
−46(13)		25(31)		Awaji 81 [41]					
		$S_{31}(1620)$ ****					$P_{33}(1920)$ ***		
−3(3)				This work	51(10)		17(15)		This work
50(2)				Dugger 07 [37]	40(14)		23(17)		Awaji 81 [41]
35(10)				Crawford 83 [40]					
35(20)				Arndt 96 [38]					
10(15)				Awaji 81 [41]					
		$D_{33}(1700)$ ****					$D_{35}(1930)$ ***		
58(10)		97(8)		This work	11(3)		2(2)		This work
160(20)		165(25)		Anisovich 12 [32]	−7(10)		5(10)		Arndt 96 [38]
125(3)		105(3)		Dugger 07 [37]	9(9)		−25(11)		Awaji 81 [41]
90(25)		97(20)		Arndt 96 [38]					
111(17)		107(15)		Crawford 83 [40]					
89(33)		60(15)		Awaji 81 [41]					
		$S_{31}(1900)$ **					$F_{37}(1950)$ ****		
−82(9)				This work	−65(1)		−83(1)		This work
59(16)				Anisovich 12 [32]	−71(4)		−94(5)		Anisovich 12 [32]
−4(16)				Crawford 83 [40]	−79(6)		−103(6)		Arndt 96 [38]
29(8)				Awaji 81 [41]	−68(7)		−94(16)		Awaji 81 [41]
					−83(8)		−92(8)		Anisovich 10 [34]
							$F_{35}(2000)$ **		
					−61(18)		158(32)		This work

pole mass is slightly smaller than those in other analyses. For $S_{31}(1900)$, both our pole mass $M_p = 1844$ MeV and the pole width $\Gamma_p = 223$ MeV are comparable to those in the analysis by Cutkosky *et al.* [8].

P$_{31}$: This partial wave was fitted with a single resonance at $M = 1934 \pm 5$ MeV with $\Gamma = 211 \pm 11$ MeV. The hadronic decay channels were found to be πN (17%), πN^* (47%), with most of the strength going into a dummy $\rho\Delta$ channel. This resonance can be identified with the 4* $P_{31}(1910)$.

The pole mass and the pole width were found to be $M_p = 1910$ MeV and $\Gamma_p = 199$ MeV, respectively. These results agree well with the analysis by Cutkosky *et al.* [8].

P$_{33}$: This partial wave was fitted with three resonances. The first resonance occurred at $M = 1231.1 \pm 0.2$ MeV with $\Gamma = 113.0 \pm 0.5$ MeV and corresponds to the 4* $P_{33}(1232)$. This state has an elasticity of 99.4%. The second resonance occurred at $M = 1626 \pm 8$ MeV with $\Gamma = 225 \pm 18$ MeV and corresponds to the 3* $P_{33}(1600)$. The major decay modes were found to be πN (8%), $\pi\Delta$ (70%), and πN^* (22%). The third resonance occurred at $M = 2146 \pm 32$ MeV with $\Gamma = 400 \pm 80$ MeV.

For $P_{33}(1232)$, the pole mass $M_p = 1212$ MeV and the pole width $\Gamma_p = 98$ MeV agree very well with previous analyses. For $P_{33}(1600)$ our pole mass $M_p = 1599$ MeV and pole width $\Gamma_p = 211$ MeV agree well with the analysis by Cutkosky *et al.* [8].

D$_{33}$: This partial wave was fitted with one resonance at $M = 1691 \pm 4$ MeV and $\Gamma = 248 \pm 9$ MeV. This state can be identified with the 4* $D_{33}(1700)$. The main hadronic decay modes were found to be πN (14%), $(\pi\Delta)_S$ (54%), and $\rho_3 N$ (30%).

The pole mass and pole width for this resonance were found to be $M_p = 1656$ MeV and $\Gamma_p = 226$ MeV, respectively. These results agree very well with previous analyses.

TABLE VIII. Comparison of decay amplitudes for $I = 1/2$ states with predictions of quark models. The first row gives our results, while the second and third rows list the available πN, ηN, $K\Lambda$, $\pi\Delta_l$, $\pi\Delta_h$, $\rho_1 N$, $\rho_3 N_l$, and $\rho_3 N_h$ amplitudes predicted by Koniuk and Isgur [46] and Capstick and Roberts [9,47], respectively. Here, the $\pi\Delta$ and ρN amplitudes by Koniuk and Isgur [46] have been multiplied by −1.

State	πN	ηN	$K\Lambda$	$\pi\Delta_l$	$\pi\Delta_h$	$\rho_1 N$	$\rho_3 N_l$	$\rho_3 N_h$
$P_{11}(1440)$	12.7(1)	–	–	+4.0(2)	–	+1.8(3)	–	–
****	6.8	–	–	+2.4	–	+0.27	–	+0.09
	$20.3^{+0.8}_{-0.9}$	$+0.0^{+1.0}_{-0.0}$	–	$+3.3^{+2.3}_{-1.8}$	–	$-0.3^{+0.2}_{-0.3}$	–	$-0.5^{+0.3}_{-0.5}$
$D_{13}(1520)$	8.55(4)	–	–	−3.3(1)	−2.7(1)	–	−4.9(1)	–
****	9.2	+0.4	–	−6.7	−2.5	+0.73	−4.98	−1.1
	8.6(3)	$+0.4^{+2.9}_{-0.4}$	$0.0^{+0.0}_{-0.9}$	$-5.7^{+3.6}_{-1.6}$	$-1.5^{+1.3}_{-3.0}$	$-0.1^{+0.1}_{-0.3}$	$-2.4^{+1.9}_{-6.4}$	$-0.3^{+0.2}_{-1.0}$
$S_{11}(1535)$	7.2(1)	+7.6(2)	–	–	+1.6(3)	−3.8(2)	–	−3.5(2)
****	5.3	+5.2	–	–	+1.7	−6.1	–	+1.6
	14.7(5)	$+14.6^{+0.7}_{-1.3}$	–	–	+1.4(3)	−0.7(1)	–	+0.4(1)
$S_{11}(1650)$	8.4(2)	−5.1(2)	−3.3(2)	–	+3.0(3)	−2.8(3)	–	−0.6(3)
****	8.7	−1.5	−3.0	–	+8.2	−9.7	–	+2.7
	12.2(8)	$-7.8^{+0.1}_{-0.0}$	$-5.2^{+1.4}_{-0.5}$	–	$+3.6^{+0.8}_{-0.6}$	$+0.9^{+0.3}_{-0.2}$	–	+0.4(1)
$D_{15}(1675)$	7.5(1)	+0.6(3)	−0.5(1)	+8.1(2)	–	+0.4(1)	−0.6(2)	–
****	5.5	−2.8	+0.1	+9.3	–	−1.1	−2.0	0
	5.3(1)	−2.5(2)	0.0	+5.7(4)	0.0	+0.2	−0.4	0.0
$F_{15}(1680)$	9.25(4)	+1.1(2)	−0.15(3)	−3.6(2)	+1.1(1)	–	−3.1(1)	−1.7(1)
****	7.1	+0.7	−0.1	−2.0	+0.7	+1.6	−3.96	−1.3
	6.6(2)	+0.6(1)	−0.1	+1.6(1)	+0.5(1)	−0.2	$-3.0^{+0.4}_{-0.5}$	−0.3(1)
$D_{13}(1700)$	1.2(1)	–	–	−4.2(8)	+1.3(5)	–	−4.6(4)	–
***	3.6	−0.7	−0.2	−16	+7.7	−0.11	−4.3	−2.74
	5.8(6)	−0.2(1)	−0.4(2)	−27.5(16)	$+4.6^{+1.6}_{-1.3}$	0.0	±0.1	$-0.9^{+0.3}_{-0.6}$
$P_{11}(1710)$	4.1(6)	−3(1)	−3.1(9)	−2.7(7)	–	−4.4(7)	–	–
***	6.7	+2.9	−2.1	−3.6	–	+5.5	–	+2.5
	4.2(1)	+5.7(3)	−2.8(6)	−13.9(15)	–	+0.3(1)	–	$-3.7^{+0.9}_{-1.2}$
$P_{13}(1720)$	5.2(3)	0.0(7)	−2.4(2)	–	–	+1.7(3)	–	–
****	6.5	+1.9	−1.7	−1.9	+1.0	+11.7	−2.6	−3.5
	14.1(1)	+5.7(3)	$-4.3^{+0.8}_{-0.7}$	−1.7(2)	$-1.0^{+0.2}_{-0.3}$	$-2.6^{+0.7}_{-0.8}$	$+1.8^{+0.6}_{-0.5}$	$+0.7^{+0.3}_{-0.2}$
$F_{15}(1860)$	6.1(3)	−3.0(7)	−0.9(2)	−1(1)	+0.1(6)	–	−2.6(10)	+8.6(9)
**	1.3	−0.6	+0.9	+7.0	+4.3	−1.7	−6.6	−4.4
	0.9(2)	−0.8(2)	−0.5(3)	$+7.8^{+0.4}_{-0.6}$	$-5.8^{+2.4}_{-3.9}$	−0.4(3)	$-7.8^{+3.1}_{-0.2}$	−0.2(1)
$D_{13}(1875)$	6(1)	–	–	−20.8(9)	−4(2)	–	+3.1(22)	–
* * *	–	–	–	–	–	–	–	–
	$8.2^{+0.7}_{-1.7}$	+4.0(2)	$-5.6^{+1.7}_{-1.3}$	$-1.4^{+0.5}_{-1.2}$	$-5.3^{+0.9}_{-0.8}$	$-4.4^{+1.9}_{-0.7}$	−6.2(24)	$-11.3^{+4.9}_{-1.6}$
$P_{11}(1880)$	9(1)	+9(2)	+13(2)	–	−2(2)	+0.3(22)	–	–
**	4.4	−0.8	−1.4	–	–	+4.6	–	−1.1
	$2.7^{+0.6}_{-0.9}$	$-3.7^{+0.5}_{-0.0}$	−0.1(1)	$-8.7^{+2.1}_{-0.4}$	–	$+2.3^{+1.7}_{-1.4}$	–	$\pm 0.3^{+0.0}_{-0.1}$
$S_{11}(1895)$	9.2(6)	+14(1)	+3.0(7)	–	+6(1)	+2.0(12)	–	−6.6(9)
**	–	–	–	–	–	–	–	–
	$5.7^{+0.5}_{-1.6}$	$+2.4^{+1.5}_{-2.3}$	+2.3(27)	–	$-6.7^{+1.5}_{-1.3}$	+2.3(6)	–	$-17.9^{+7.3}_{-3.8}$
$P_{13}(1900)$	2.6(8)	0.0(8)	−3.7(6)	–	–	+8.0(6)	–	–
* * *	3.2	−2.9	–	+4.1	+1.5	−0.43	−1.32	−0.46
	$6.1^{+0.6}_{-1.2}$	−4.6(3)	$-0.9^{+0.4}_{-0.1}$	+3.8(5)	$-2.2^{+1.2}_{-1.5}$	$-1.4^{+0.9}_{-1.0}$	−1.0(6)	$+0.2^{+0.5}_{-0.2}$
$F_{17}(1990)$	2.1(6)	–	−1.0(5)	–	–	–	–	–
**	3.1	−2.3	−0.3	+6.0	–	−0.80	+4.2	0
	2.4(4)	$-2.2^{+0.6}_{-0.7}$	0.0	$+5.0^{+2.0}_{-1.4}$	0.0	+0.6(3)	$-1.0^{+0.6}_{-0.5}$	0.0
$D_{15}(2060)$	5(1)	+0.6(15)	+0.3(20)	+11(2)	–	−7.9(25)	−3.5(18)	–
**	–	–	–	–	–	–	–	–
	$5.2^{+0.4}_{-1.0}$	$+0.0^{+0.4}_{-0.2}$	$-1.7^{+0.5}_{-0.4}$	$+7.8^{+1.1}_{-1.3}$	$+0.9^{+0.8}_{-0.4}$	$-0.8^{+0.3}_{-0.4}$	$+0.8^{+0.6}_{-0.4}$	$+2.1^{+2.4}_{-1.2}$
$G_{17}(2190)$	10.0(9)	−3(1)	+0.3(4)	–	–	–	−6.7(24)	–
****	–	–	–	–	–	–	–	–
	6.9(13)	+2.5(7)	$-1.3^{+0.4}_{-0.6}$	−1.3(2)	$-2.6^{+0.9}_{-1.3}$	$-1.9^{+0.7}_{-1.5}$	$-11.4^{+1.0}_{-3.8}$	$-3.7^{+1.4}_{-3.0}$

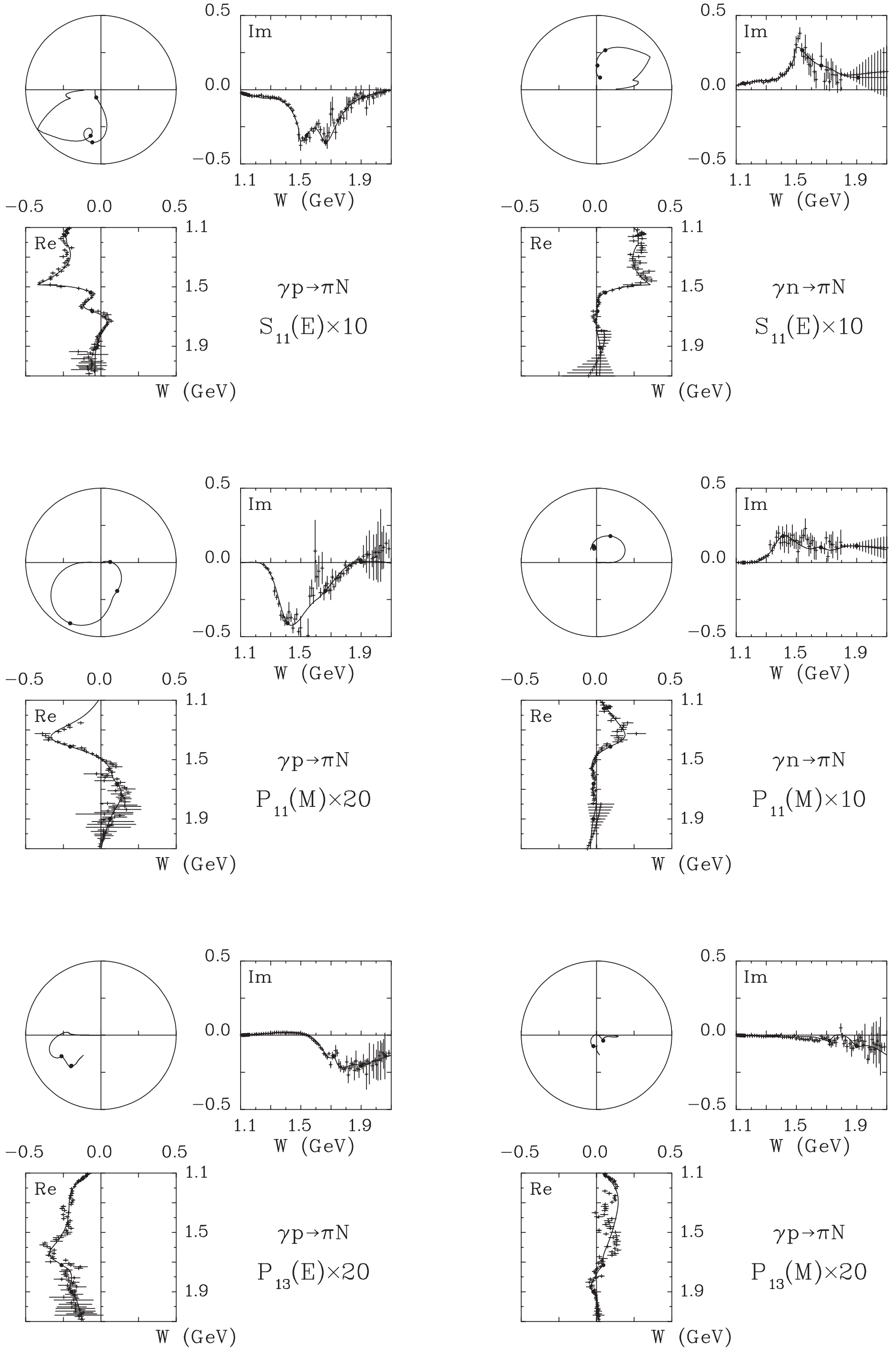

FIG. 6. Argand diagrams for pion-photoproduction amplitudes.

$\mathbf{D_{35}}$: This partial wave was fitted with one resonance at $M = 1930 \pm 14$ MeV with $\Gamma = 235 \pm 39$ MeV. This resonance can be identified with the 3* $D_{35}(1930)$. This state was found to have an elasticity of only 8% with all the inelasticity carried by the dummy $\rho\Delta$ channel.

The pole mass and the pole width for this resonance were found to be $M_p = 1882$ MeV and $\Gamma_p = 187$ MeV, respectively. These values agree very well with analyses by Höhler [31] and Cutkosky *et al.* [8] but are smaller than those in the analysis by Arndt *et al.* [12].

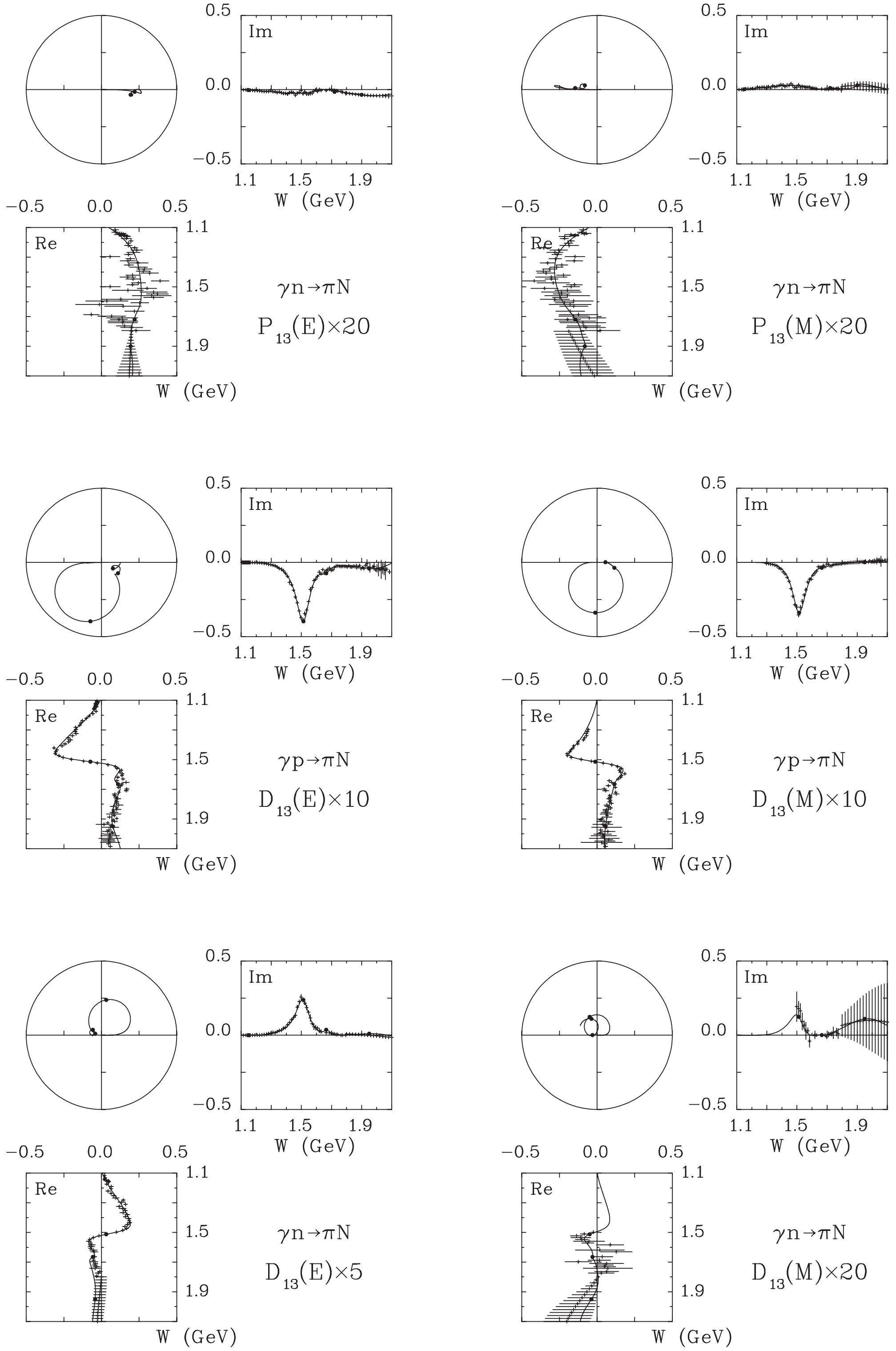

FIG. 7. Same as in Fig. 6.

F_{35}: This partial wave was fitted with two resonances. The first resonance occurred at $M = 1818 \pm 8$ MeV with $\Gamma = 278 \pm 18$ MeV. This resonance can be identified with the 4* $F_{35}(1905)$. Its major hadronic decay channels were found to be πN (6%), $(\pi\Delta)_P$ (28%), and $(\pi\Delta)_F$ (64%). The second resonance occurred at $M = 2015 \pm 24$ MeV with $\Gamma = 500 \pm 52$ MeV. Its major decay modes were found to be πN (7%), $(\pi\Delta)_P$ (3%), and $\rho_3 N$ (90%). This state corresponds to the 2* $F_{35}(2000)$.

The pole mass and the pole width for $F_{35}(1905)$ were found to be $M_p = 1769$ MeV and $\Gamma_p = 239$ MeV, respectively. This pole mass is somewhat smaller than that in previous analyses

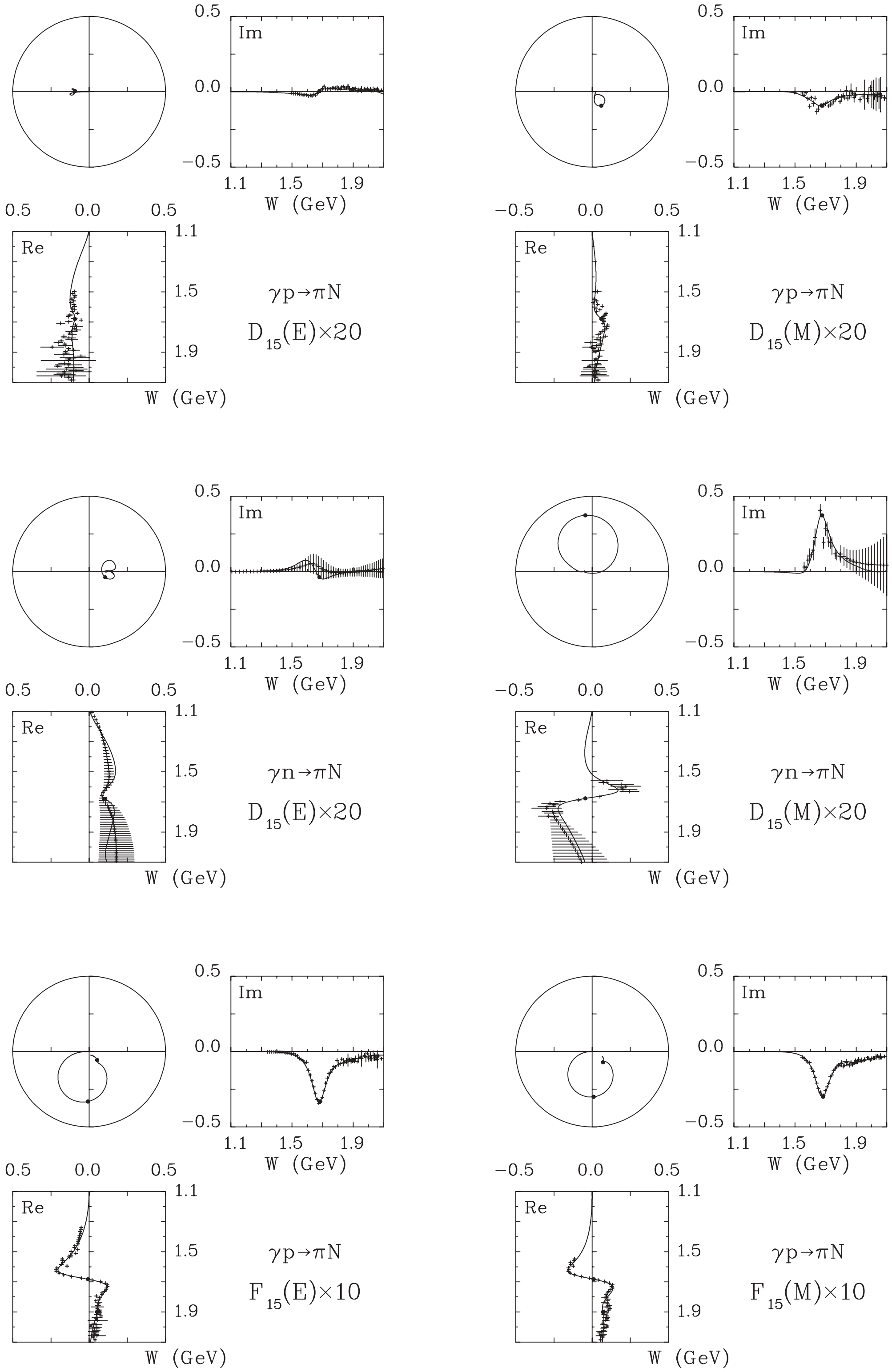

FIG. 8. Same as in Fig. 6.

but the pole width is comparable with that by Arndt *et al.* [12]. The pole mass and the pole width for $F_{35}(2000)$ were found to be $M_p = 1976$ MeV and $\Gamma_p = 488$ MeV, respectively. These results are comparable with those by Cutkosky *et al.* [8] but larger than the values presented in the analysis by Vrana *et al.* [26].

$\mathbf{F_{37}}$: This partial wave was fitted with one resonance at $M = 1918 \pm 1$ MeV with $\Gamma = 259 \pm 4$ MeV. This state can be identified with the 4* $F_{37}(1950)$. This state was found to have an elasticity of 46%. Most of the inelasticity was carried by a dummy $\rho\Delta$ channel while about 8% was found to be associated with the $\pi\Delta$ channel.

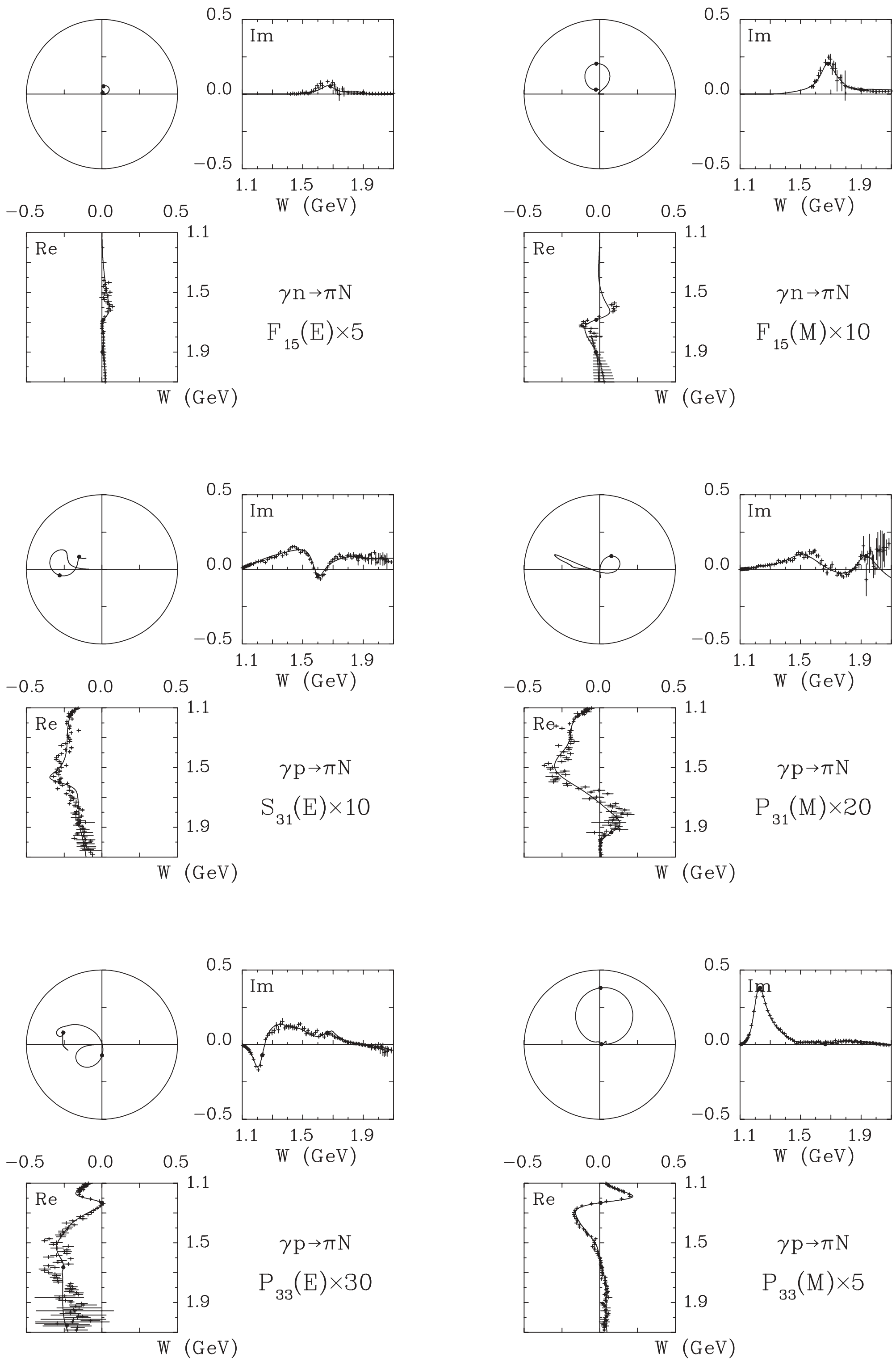

FIG. 9. Same as in Fig. 6.

The pole mass and the pole width were found to be $M_p = 1871$ MeV and $\Gamma_p = 220$ MeV, respectively. Theses results agree very well with previous analyses.

In Table VII we present our results on helicity amplitudes for $I = 1/2$ and $I = 3/2$ states, and compare these results with those from earlier analyses. The first column lists the resonance name. The second and third columns list the helicity-$1/2$ amplitudes for proton and neutron targets, respectively, and the fourth and fifth columns list the helicity-$3/2$ amplitudes for proton and neutron targets, respectively. Our results on helicity amplitudes, in most cases, are comparable both in magnitude and sign with previous

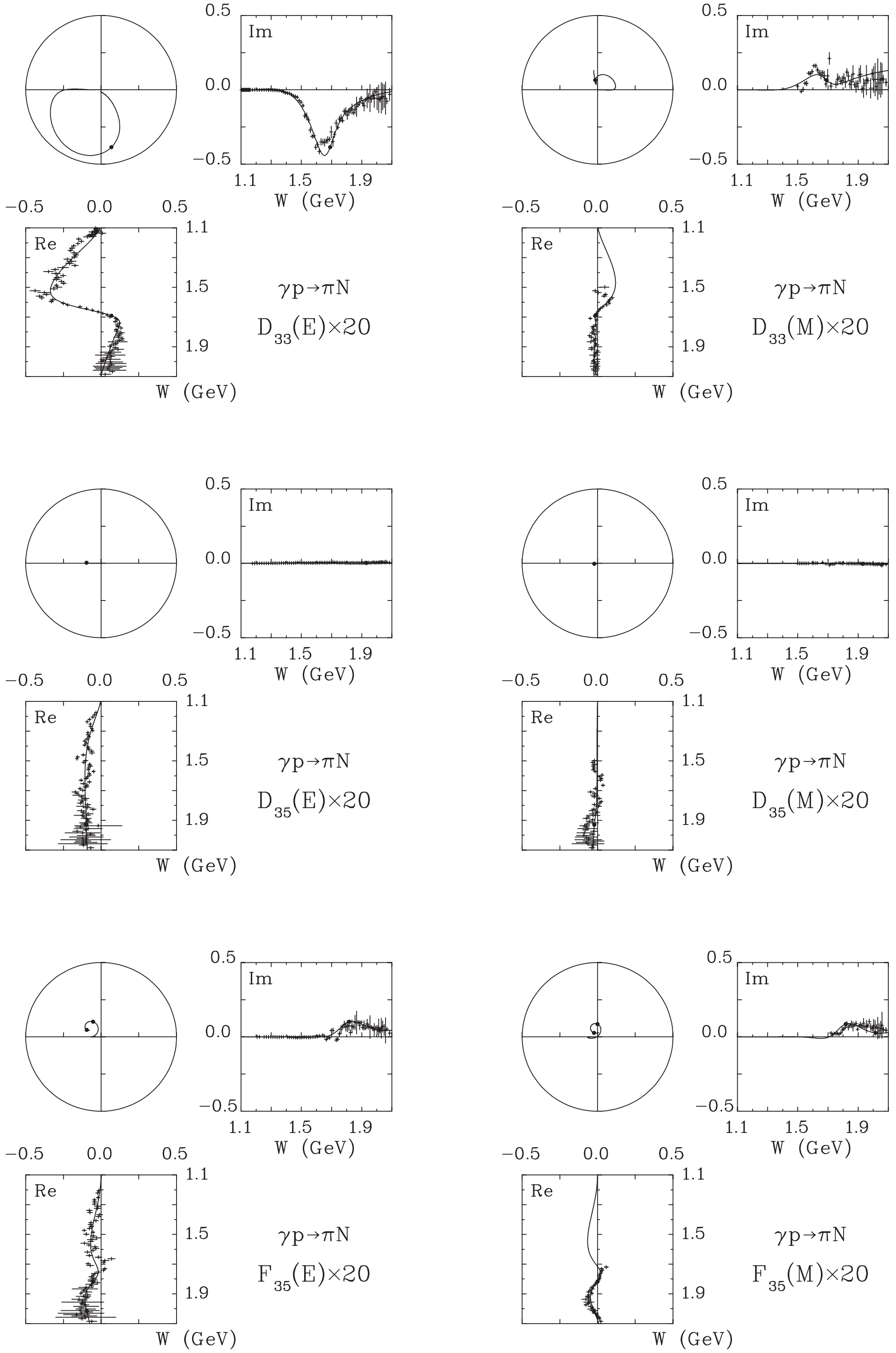

FIG. 10. Same as in Fig. 6.

analyses. For $P_{11}(1880)$, our result for the proton target agrees quite well with the solution "b" of the analysis by Anisovich *et al.* [32] but disagrees in sign with the solution "a". Resonances where we differ significantly with previous analyses are seen to be $S_{11}(1650)$, $S_{31}(1620)$, $P_{33}(1600)$, and $F_{35}(1905)$. For $S_{11}(1650)$, the helicity-1/2 amplitude for the neutron target was found to be $+0.011$ GeV$^{-1/2}$, which differs in sign and is considerably smaller than the values in analyses by Anisovich *et al.* [35] and Arndt *et al.* [12]. The same is true for $S_{31}(1620)$ and $P_{33}(1600)$ with our helicity amplitudes of -0.003 and $+0.006$ GeV$^{-1/2}$, respectively. For $F_{35}(1905)$ our helicity-1/2 and helicity-3/2 amplitudes are considerably larger than in other analyses although we agree in sign.

Figures 6–11 show representative Argand diagrams for pion photoproduction amplitudes ($\gamma N \to \pi N$) for both $I = 1/2$ and $I = 3/2$ partial waves. These amplitudes are dimensionless unlike those from Ref. [12], which are expressed in milli-fermi (mfm). Details of the conversion from dimensioned amplitudes to our dimensionless amplitudes can be found elsewhere [19,36].

V. COMPARISONS WITH QUARK-MODEL PREDICTIONS

In Tables VIII and IX we present decay amplitudes for various channels and compare our results for $I = 1/2$ and $I = 3/2$ states, respectively, with quark models. The magnitude of the decay amplitude is equal to $\sqrt{\Gamma_i}$, the square root of the partial width for the channel. Its sign is the phase relative to the πN coupling (taken to be positive). The values in the first row are our results, while those in the second row are from Koniuk and Isgur [46] and the third from Capstick and Roberts [9,47]. The channels included are πN, ηN, $K\Lambda$, $\pi\Delta$, and ρN. The subscript 'l' or 'h' that appears with a channel represents the lower or higher orbital angular momentum of that channel. The states are listed in the first column in an ascending order in terms of their masses.

On comparing with predictions of quark models we find that our results over-all agree well with either one or both models. If we break down channel by channel, we have excellent agreements for the elastic decay amplitudes with at least one of the quark models for all states except $D_{13}(1700)$

TABLE IX. Comparison of decay amplitudes for $I = 3/2$ states with predictions of quark models. The first row gives our results, while the second and third rows list the available πN, $\pi\Delta_l$, $\pi\Delta_h$, $\rho_1 N$, $\rho_3 N_l$, and $\rho_3 N_h$ amplitudes predicted by Koniuk and Isgur [46] and Capstick and Roberts [9,47], respectively. Here, the $\pi\Delta$ and ρN amplitudes by Koniuk and Isgur [46] have been multiplied by -1.

State	πN	$\pi\Delta_l$	$\pi\Delta_h$	$\rho_1 N$	$\rho_3 N_l$	$\rho_3 N_h$
$P_{33}(1232)$	10.60(2)	0.00(5)	–	–	–	–
****	11.0	–	–	–	–	–
	10.4(1)	–	–	–	–	–
$P_{33}(1600)$	4.2(5)	+12.5(4)	–	–	–	–
***	5.4	+8.6	+0.1	−1.3	−5.5	−0.35
	8.7(2)	$+8.4^{+3.6}_{-3.5}$	0.0	$+0.4^{+0.7}_{-0.3}$	$-0.9^{+0.6}_{-1.4}$	0.0
$S_{31}(1620)$	6.1(1)	–	−6.0(2)	+5.4(2)	–	−0.6(2)
****	3.3	–	−8.0	+7.82	–	−1.72
	5.1(7)	–	$-4.2^{+1.3}_{-1.8}$	$-3.6^{+1.3}_{-2.5}$	–	$-0.3^{+0.1}_{-0.2}$
$D_{33}(1700)$	6.0(2)	+11.6(3)	+1.9(6)	–	+8.7(4)	–
****	4.9	+10.3	+6.3	+4.2	+16.5	+0.89
	4.9(7)	$+15.4^{+0.9}_{-1.8}$	$+5.0^{+2.4}_{-1.8}$	$-1.2^{+0.6}_{-1.2}$	$+3.4^{+2.2}_{-1.7}$	$+0.5^{+0.5}_{-0.2}$
$S_{31}(1900)$	4.4(5)	–	−11.5(8)	−5.4(9)	–	−7.3(10)
**	–	–	–	–	–	–
	$3.1^{+0.4}_{-1.1}$	–	$-4.4^{+0.8}_{-0.7}$	−2.2(6)	–	$+2.3^{+1.0}_{-0.4}$
$F_{35}(1905)$	4.0(3)	+8.8(11)	+13.3(10)	–	−2.6(14)	–
****	4.0	+3.2	+5.5	−0.049	−2.1	−6.4
	3.4(3)	−1.5	+4.7(6)	−0.7(2)	$+6.3^{+0.8}_{-0.4}$	$-0.7^{+0.1}_{-0.2}$
$P_{31}(1910)$	6.0(2)	–	–	–	–	–
****	5.3	+5.9	–	−3.7	–	−4.9
	9.4(4)	$-8.4^{+0.2}_{-0.1}$	–	$+5.6^{+0.9}_{-0.4}$	–	$+2.6^{+0.4}_{-0.2}$
$P_{33}(1920)$	7.9(12)	−5.2(21)	–	–	–	–
***	5.2	−3.2	−1.4	−8.1	+6.2	+5.5
	4.2(3)	$-8.9^{+0.3}_{-0.2}$	$+4.4^{+0.8}_{-0.7}$	$+5.3^{+1.3}_{-0.5}$	$+6.6^{+1.6}_{-0.7}$	$-0.7^{+0.2}_{-0.4}$
$D_{35}(1930)$	4.3(4)	–	–	–	–	–
* * *	–	–	–	–	–	–
	5.2(1)	+3.9(2)	−0.7(1)	+0.1	$-2.9^{+0.5}_{-0.8}$	$-0.1^{+0.0}_{-0.1}$
$F_{37}(1950)$	10.9(1)	+4.7(3)	–	–	–	–
****	7.5	+5.5	0.0	−4.69	−8.2	0
	7.1(1)	+4.8(2)	0.0	+1.3(1)	−2.3(2)	0.0
$F_{35}(2000)$	5.8(5)	−3.7(17)	+1.7(29)	–	+21.2(12)	–
**	1.0	−6.2	+1.4	+7.2	+17.8	+4.6
	1.2(3)	$-14.0^{+1.6}_{-0.1}$	$+1.5^{+1.5}_{-0.8}$	$+2.6^{+2.8}_{-2.1}$	+3.1(12)	$-3.1^{+2.4}_{-3.2}$

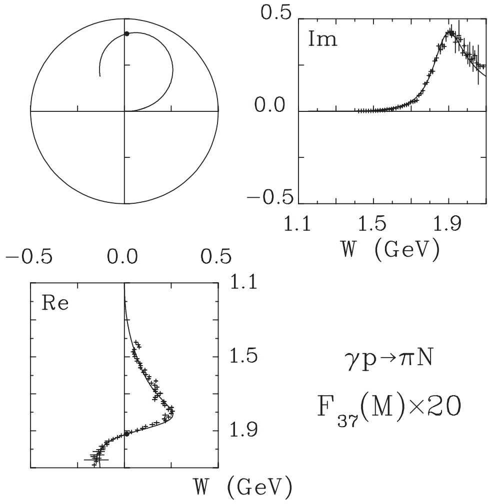

FIG. 11. Same as in Fig. 6.

and $F_{15}(1860)$. For $F_{15}(1860)$ our πN amplitude of 6.1 is larger than the model values of 1.3. For $D_{13}(1700)$ our elastic coupling of 1.2 is smaller than the model values of 3.6 and 5.8.

The predicted ηn and $K\Lambda$ decay amplitudes for $D_{13}(1520)$ and $D_{13}(1700)$ are small, in agreement with our results.

Our ηN results are in excellent agreement with the model predictions for $S_{11}(1535)$, $S_{11}(1650)$, and $F_{15}(1680)$. For $P_{11}(1710)$ and $G_{17}(2190)$, our ηN results agree very well in magnitude but not in sign with the predictions. The states for which our ηN results agree in sign but not in magnitude with the predictions are $P_{13}(1720)$, $P_{11}(1880)$, $S_{11}(1895)$, and $F_{17}(1990)$. For $D_{15}(1675)$, our ηN amplitude (+0.6) disagrees both in magnitude and sign with model predictions (−2.8 and −2.5).

Our $K\Lambda$ results are in excellent agreement with the predictions for $S_{11}(1650)$, $F_{15}(1680)$, $P_{11}(1710)$, $P_{13}(1720)$, $S_{11}(1895)$, and $F_{17}(1990)$. For $F_{15}(1860)$, our $K\Lambda$ results agree very well in magnitude but not in sign with model predictions. For $P_{11}(1880)$ and $P_{13}(1900)$ there are no predictions with which to compare our $K\Lambda$ results. For $G_{17}(2190)$ our $K\Lambda$ amplitude (+0.3) disagrees both in magnitude and sign with the model prediction of −1.3 by Capstick and Roberts [47].

The excellent agreement of our $K\Lambda$ results with model predictions can be attributed to the extensive and nonproblematic $K\Lambda$ database. The less extensive and more problematic ηN data, especially by Brown *et al.*, could be the reason for the poorer agreement of our ηN results with model predictions.

Our results confirm the existence of $P_{11}(1710)$ and are further supported by the excellent agreements of our $K\Lambda$ and ηN amplitudes with predictions of quark models [9,47].

In Table X we compare our helicity amplitudes (in units of 10^{-3} GeV$^{-1/2}$) with model predictions by Koniuk and Isgur [46] (second row) and by Capstick [48] (third row). For $P_{33}(1232)$, $D_{13}(1520)$, $D_{15}(1675)$, $F_{15}(1680)$, and $F_{37}(1950)$

TABLE X. Comparison of helicity amplitudes with predictions of quark models. The first row lists our results, while the second and third rows list the helicity amplitudes predicted by Koniuk and Isgur [46] and Capstick [48], respectively. The first column identifies the states.

State	$A^p_{1/2}$	$A^n_{1/2}$	$A^p_{3/2}$	$A^n_{3/2}$	State	$A^p_{1/2}$	$A^n_{1/2}$	$A^p_{3/2}$	$A^n_{3/2}$
$P_{11}(1440)$	−84(3)	40(5)	–	–	$P_{13}(1720)$	57(3)	−2(1)	−19(2)	−1(2)
****	−24	16	–	–	****	−133	57	46	−10
	4	−6	–	–		−11	4	−31	11
$D_{13}(1520)$	−34(1)	−38(3)	127(3)	−101(4)	$P_{33}(1232)$	−137(1)	–	−251(1)	–
****	−23	−45	128	−122	****	−103	–	−179	–
	−15	−38	134	−114		−108	–	−108	–
$S_{11}(1535)$	59(3)	−49(3)	–	–	$P_{33}(1600)$	6(5)	–	52(8)	–
****	147	−119	–	–	***	−16	–	−46	–
	76	−63	–	–		30	–	51	–
$S_{11}(1650)$	30(3)	11(2)	–	–	$S_{31}(1620)$	−3(3)	–	–	–
****	88	−35	–	–	****	59	–	–	–
	54	−35	–	–		81	–	–	–
$D_{15}(1675)$	11(1)	−40(4)	20(1)	−68(4)	$D_{33}(1700)$	58(10)	–	97(8)	–
****	12	−37	16	−53	****	100	–	105	–
	2	−35	3	−51		82	–	68	–
$F_{15}(1680)$	−17(1)	29(2)	136(1)	−59(2)	$F_{35}(1905)$	68(18)	–	−223(29)	–
****	∼0	26	91	−25	****	8	–	−33	–
	−38	19	56	−23		26	–	−1	–
$D_{13}(1700)$	21(5)	−49(8)	50(9)	−92(14)	$P_{31}(1910)$	30(2)	–	–	–
***	−7	−15	11	−76	****	∼0	–	–	–
	−33	18	−3	−30		−8	–	–	–
$P_{11}(1710)$	−8(3)	17(3)	–	–	$F_{37}(1950)$	−65(1)	–	−83(1)	–
***	−47	−21	–	–	****	−50	–	−69	–
	13	−11	–	–		−33	–	−42	–

our results are in excellent agreement both in magnitude and sign with the predictions. For $P_{11}(1440)$, $S_{11}(1535)$, and $F_{35}(1905)$ our results agree with predictions in sign but not in magnitude. For the remaining states our results differ in sign or magnitude with model predictions for one or more helicity amplitudes. It is of interest to ask whether or not our results can shed any light on a recent puzzle involving η photoproduction. Precise data measured at Bonn using quasi-free scattering from deuterium have revealed a narrow peak in the cross section for $\gamma n \to \eta n$ at $W \simeq 1665$ MeV [49]. This structure is not observed in $\gamma p \to \eta p$. A more recent analysis [50] has shown that this peak is a bit wider than originally reported. If this peak is associated with an N^* resonance, then only the $D_{13}(1700)$ in our analysis has a mass and width consistent with newer results for the state seen in $\gamma n \to \eta n$. Interestingly, we find that the γn couplings for $D_{13}(1700)$ are about twice as large as its γp couplings, so if this state has a nonzero coupling to ηN, it is reasonable that it might be seen in $\gamma n \to \eta n$ but not in $\gamma p \to \eta p$.

VI. SUMMARY AND CONCLUSIONS

This work was undertaken to determine the parameters of N^* and Δ^* resonances with masses up to about 2.1 GeV using a global multichannel fit. For the first time, we explicitly include amplitudes for $\pi N \to \eta N$ and $\pi N \to K\Lambda$ in addition to those for $\pi N \to \pi N$, $\pi N \to \pi\pi N$, and $\gamma N \to \pi N$. Most resonance parameters determined from this work agree satisfactorily with previous analyses [8,12,18,28]. We find significant couplings of $S_{11}(1650)$ and $P_{11}(1710)$ to both ηN and $K\Lambda$. These results confirm the existence of $P_{11}(1710)$, for which no evidence was found in the analysis by Arndt *et al.* [12]. Also our work finds considerable couplings of $P_{13}(1900)$ to πN and $K\Lambda$. Our results, on the whole, agree well with the predictions of quark models [9,46,47].

It is worthwhile to compare our results with the recent multichannel analysis by Anisovich *et al.* [32]. Their analysis claims the existence of a number of new states. Interestingly we find all resonances listed in their analysis with masses below about 2100 MeV. Moreover, we find two additional resonances $D_{35}(1930)$ and $F_{35}(2000)$. The other difference is we obtain both γp and γn helicity couplings while their analysis gives only γp couplings. We have good agreement with their results for $P_{11}(1880)$, $F_{15}(1860)$, $P_{13}(1900)$, and $D_{15}(2060)$, which strengthens the evidence for these newly proposed states.

ACKNOWLEDGMENTS

This work was supported by US Department of Energy Grant No. DE-FG02-01ER41194. The authors thank the GWU group and especially Igor Strakovsky for providing part of the database for $\pi^- p \to \eta n$.

[1] N. Isgur and G. Karl, Phys. Rev. D **19**, 2653 (1979); **23**, 817(E) (1981).
[2] S. Capstick and N. Isgur, Phys. Rev. D **34**, 2809 (1986).
[3] L. Y. Glozman, W. Plessas, K. Varga, and R. F. Wagenbrunn, Phys. Rev. D **58**, 094030 (1998).
[4] U. Löring, B. Ch. Metsch, and H. R. Petry, Eur. Phys. J. A **10**, 395 (2001).
[5] S. Capstick and W. Roberts, Prog. Part. Nucl. Phys. **45**, S241 (2000).
[6] J. Beringer *et al.* (Particle Data Group), Phys. Rev. D **86**, 010001 (2012).
[7] R. A. Arndt, Z. Li, L. D. Roper, R. L. Workman, and J. M. Ford, Phys. Rev. D **43**, 2131 (1991).
[8] R. E. Cutkosky, C. P. Forsyth, R. E. Hendrick, and R. L. Kelly, Phys. Rev. D **20**, 2839 (1979); R. E. Cutkosky, C. P. Forsyth, J. B. Babcock, R. L. Kelly, and R. E. Hendrick, in *Baryons 1980*, Proceedings of the 9th International Conference on Baryon Resonances, Toronto, Canada, edited by N. Isgur (University of Toronto, Toronto, 1980), p. 19.
[9] S. Capstick and W. Roberts, Phys. Rev. D **49**, 4570 (1994).
[10] B. Julia-Diaz, T. S. H. Lee, A. Matsuyama, and T. Sato, Phys. Rev. C **76**, 065201 (2007).
[11] A. Sarantsev, Chinese Phys. C **33**, 1085 (2009).
[12] R. A. Arndt, W. J. Briscoe, I. I. Strakovsky, and R. L. Workman, Phys. Rev. C **74**, 045205 (2006).
[13] F. Huang *et al.*, Phys. Rev. C **85**, 054003 (2012).
[14] M. Shrestha and D. M. Manley, Phys. Rev. C **86**, 045204 (2012).
[15] M. Shrestha, Ph.D. dissertation, Kent State University, 2012.
[16] D. M. Manley, Int. J. Mod. Phys. A **18**, 441 (2003).
[17] T.-S. H. Lee, in *NSTAR 2005*, Proceedings of the Workshop on the Physics of Excited Nucleons, edited by S. Capstick, V. Crede, and P. Eugenio (World Scientific, Singapore, 2006), p. 1.
[18] D. M. Manley and E. M. Saleski, Phys. Rev. D **45**, 4002 (1992).
[19] M. M. Niboh, Ph.D. dissertation, Kent State University, 1997.
[20] J. Tulpan, Ph.D. dissertation, Kent State University, 2007.
[21] H. Zhang, Ph.D. dissertation, Kent State University, 2008.
[22] R. A. Arndt, private communication (2007).
[23] D. M. Manley, R. A. Arndt, Y. Goradia, and V. L. Teplitz, Phys. Rev. D **30**, 904 (1984).
[24] GWU Center for Nuclear Studies Data Analysis Center http://gwdac.phys.gwu.edu.
[25] V. V. Abaev and B. M. K. Nefkens, Phys. Rev. C **53**, 385 (1996).
[26] T. P. Vrana, S. A. Dytman, and T.-S. H. Lee, Phys. Reports **328**, 181 (2000).
[27] D. H. Saxon *et al.*, Nucl. Phys. B **162**, 522 (1980).
[28] G. Höhler *et al.*, Physik Daten 12-1 (1979).
[29] M. Batinić, I. Šlaus, A. Švarc, and B. M. K. Nefkens, Phys. Rev. C **51**, 2310 (1995).
[30] R. E. Cutkosky and S. Wang, Phys. Rev. D **42**, 235 (1990).
[31] G. Höhler, in *Proceedings of the 5th International Symposium on Meson-Nucleon Physics and the Structure of the Nucleon, Boulder, CO*, Vol. II, edited by B. M. K. Nefkens and M. Clajus (πN Newsletter No. 9, 1993), p. 1.
[32] A. V. Anisovich *et al.*, Eur. Phys. J. A **48**, 15 (2012).
[33] R. S. Longacre, T. Lasinski, A. H. Rosenfeld, G. Smadja, R. J. Cashmore, and D. W. G. S. Leith, Phys. Rev. D **17**, 1795 (1978).
[34] A. V. Anisovich, Eur. Phys. J. A **44**, 203 (2010).

[35] A. V. Anisovich, Eur. Phys. J. A **41**, 13 (2009).
[36] D. M. Manley, in *Proceedings of the GW/JLab Workshop on N* Physics, Ashburn, VA*, edited by H. Habertzettl, C. Bennhold, and W. J. Briscoe (πN Newsletter No. 14, 1998), p. 158.
[37] M. Dugger *et al.* (CLAS Collaboration), Phys. Rev. C **76**, 025211 (2007); **79**, 065206 (2009).
[38] R. A. Arndt, I. I. Strakovsky, and R. L. Workman, Phys. Rev. C **53**, 430 (1996).
[39] J. Ahrens *et al.*, Phys. Rev. Lett. **88**, 232002 (2002).
[40] R. L. Crawford and W. T. Morton, Nucl. Phys. B **211**, 01 (1983).
[41] N. Awaji *et al.*, in *Proceedings of the 10th International Symposium on Lepton and Photon Interactions at High Energy, Bonn, Germany*, edited by W. Pfeil (University of Colorado, Boulder, 1981), p. 352.
[42] B. Krusche, N. C. Mukhopadhyay, and J. F. Zhang, Phys. Lett. B **397**, 171 (1997).
[43] M. Benmerrouche, N. C. Mukhopadhyay, and J. F. Zhang, Phys. Rev. D **51**, 3237 (1995).
[44] K. Fujii *et al.*, Nucl. Phys. B **187**, 53 (1981).
[45] R. A. Arndt, W. J. Briscoe, I. I. Strakovsky, and R. L. Workman, Phys. Rev. C **66**, 055213 (2002).
[46] R. Koniuk and N. Isgur, Phys. Rev. D **21**, 1868 (1980); R. Koniuk, Nucl. Phys. B **195**, 452 (1982).
[47] S. Capstick and W. Roberts, Phys. Rev. D **58**, 074011 (1998).
[48] S. Capstick, Phys. Rev. D **46**, 2864 (1992).
[49] I. Jaegle *et al.*, Eur. Phys. J. A **47**, 89 (2011).
[50] D. Werthmueller, talk presented at Crystal Ball Collaboration Meeting, Mainz, Germany, Sept. 8, 2012.